Task Report 3 – Material Characterization

Project Title: Relative Operational Performance of Geosynthetics Used as Subgrade Stabilization

Submitted By: Eli Cuelho, P.E., Research Engineer
Western Transportation Institute, Montana State University – Bozeman

Dr. Steven Perkins, P.E., Professor in Civil Engineering
Civil Engineering Department, Montana State University – Bozeman

Zachary Morris, Research Associate
Western Transportation Institute, Montana State University – Bozeman

Submitted to: Craig Abernathy, Project Manager
Montana Department of Transportation, Research Programs

Date Submitted: August 20, 2013

Introduction

Various laboratory tests were used to characterize the three primary materials used to construct the field experiment associated with this project: artificial subgrade soil, base course aggregate, and geosynthetics. A general overview of the material properties of the subgrade and base course was provided in Task Report 1, and a detailed summary of the constructed properties of the subgrade and base course was provided in Task Report 2. While Task Report 2 provided a general overview of the geosynthetic characteristics as provided in manufacturer's data sheets, several other material tests were conducted by Western Transportation Institute (WTI) and an outside testing lab to further characterize these materials. These material properties will be used in the analysis of the results to determine their potential relationship to the performance of the test sections. The results of five laboratory tests are discussed in this task report and include wide-width tensile strength (ASTM D4595 and ASTM D6637), cyclic tensile modulus (ASTM D7556), resilient interface shear stiffness (ASTM D7499), junction strength (ASTM D7737), and aperture stability modulus (Kinney, 2000). The first three tests were performed by WTI and the last two tests were conducted by SGI Testing Services (Norcross, GA), an independent geosynthetic testing lab. All of the testing by WTI and SGI was performed in general accordance with the test's respective testing standard, and any deviations from the standard are noted in the subsections below.

Wide-Width Tensile Strength

The wide-width tensile strength test is used to determine the force-elongation curve of the geosynthetic in its two principal directions. A MTS servo-hydraulic load frame was used to conduct the wide-width tensile testing. The geosynthetics were held on both ends by Curtis Sure-Grip Geosynthetic Grips which apply pressure to the geosynthetics using a pneumatically driven hydraulic system. The grips can accommodate a sample up to 8 inches wide and have a capacity of 10,000 lbs. The setup for a typical wide-width tensile test is shown in Figure 1.

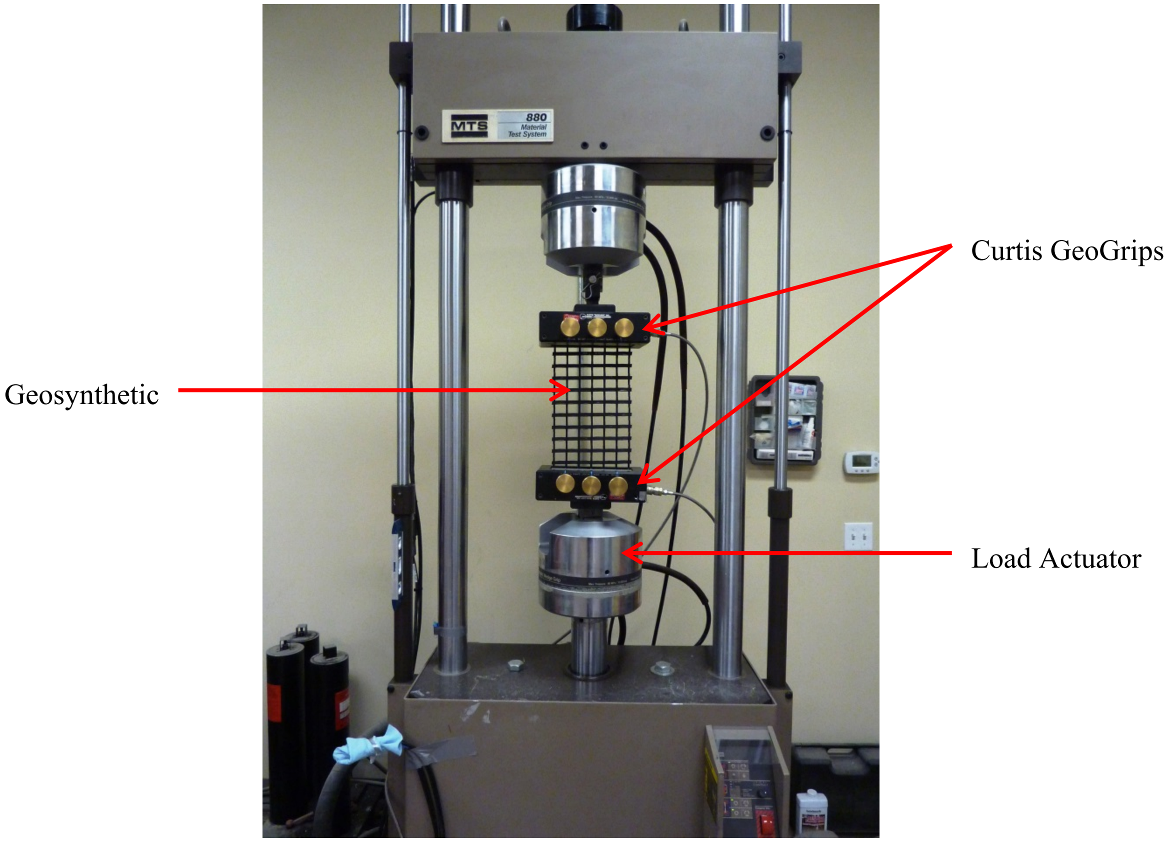

Figure 1: Wide-width tensile strength test setup.

The geogrid test samples were approximately eight inches wide and had a gage length of approximately twelve inches long, while the geotextile test samples had a width of eight inches and gage length of four inches. Tension was applied at a constant rate of strain of 10% per minute based off of the initial gage length of the geosynthetic At least three samples, but no more than six, were tested in both the machine direction (MD) and cross-machine direction (XMD). The number of samples tested is based upon a statistical formula within the standard test methods to ensure uniformity of results.

A summary of the test results from WTI and the wide-width tensile results published by the manufacturer are listed in Table 1. For the most part, strength values exceeded MARV (minimum average roll value) results published by the manufacturer; however, some materials exhibited lower values. Individual load-displacement plots are provided in Appendix A.

Table 1: Summary of Wide-Width Tensile Strength Test Results

Geosynthetic Test Section	Tested by WTI						Published by Manufacturer					
	Strength[a] @ 2% (lb/ft)		Strength[a] @ 5% (lb/ft)		Ultimate[a] Strength (lb/ft)		Strength[a,b] @ 2% (lb/ft)		Strength[a,b] @ 5% (lb/ft)		Ultimate[a,b] Strength (lb/ft)	
	MD	XMD	MD	XMD	MD	XMD	MD	XMD	MD	XMD	MD	XMD
Tensar BX Type 2	582	822	1,076	1,494	1,480	1,946	410	620	810	1,340	1,310	1,970
NAUE Secugrid 30/30 Q1	966	946	1,809	1,830	2,083	2,713	686	686	1,475	1,475	2,055	2,055
Colbond Enkagrid Max 30	1,000	857	2,028	1,775	2,645	2,378	754	754	1,576	1,576	2,056	2,056
Synteen SF 11	397	617	685	925	2042[c]	3782[c]	526	578	792	1,042	2,388	3,870
Synteen SF 12	397	987	713	1,446	2145[c]	5818[c]	526	797	1,042	1,367	2,388	5,268
TenCate Mirafi BXG 11	644	740	1,377	1,281	2,631	3,221	625	625	1,000	1,000	2,500	2,500
Huesker Fornit 30	665	946	1,425	1,939	1,864	2,618	548	890	1,370	1,850	1,850	2,398
SynTec Tenax MS330[d]	569	692	1,048	1,343	1,412	2,248	418	620	925	1,343	1,370	2,100
Tensar TX 140	34	322	178	665	624	843	NP		NP		NP	
Tensar TX 160	69	391	260	747	754	884	NP		NP		NP	
TenCate Mirafi RS580i	500	1,501	1,288	3,440	5,619	6,112	NP		NP		NP	
Propex Geotex 801	[e]		[e]		149[f]	87[f]	NP		NP		205[g]	

[a] ASTM D4595 or ASTM D6637
[b] Manufacturers' minimum average roll values (MARV)
[c] Synteen SF 11 and Synteen SF 12 materials experienced some grip slippage at their ultimate strength values
[d] Tested by WTI as a composite, i.e., not separately
[e] Data was difficult to interpret at low strain values
[f] Grab tensile strength (ASTM D-4632) in Pounds at 50% elongation as tested by SGI Testing Services, LLC
[g] Grab tensile strength (ASTM D-4632) in Pounds at 50% elongation (weaker principal direction)
NP = Information was not provided by the manufacturer

Cyclic Tensile Modulus

The cyclic tensile modulus test used the same setup as the wide-width tensile strength test (i.e., grips, testing frame, and sample sizes). These tests were performed to evaluate the tensile modulus of geosynthetics for applications involving small-strain cyclic loading (representative of traffic loads) according to ASTM D7556. The test is used to determine the cyclic tensile modulus at various levels of permanent strain. The test procedure applies 1000 cycles at 1 Hz between axial strain limits of ±0.1 percent at six permanent strain values: 0.5, 1.0, 1.5, 2.0, 3.0, and 4.0 percent. The total number of tests is determined using the same statistical equation as the wide-width tensile strength test to ensure uniformity of results.

The cyclic tensile modulus (J_{cyclic}) is calculated using the following equations:

$$J_{cyclic} = \frac{(\alpha_f * 100)}{(\varepsilon_2 - \varepsilon_1)} \qquad \text{Equation 1}$$

where α_f = the equivalent force per unit width (lb/ft), as determined using the following equation,

$$\alpha_f = \frac{(P_2 - P_1)}{W_s} \qquad \text{Equation 2}$$

ε_2 = percent strain corresponding to the cycle's highest strain value,
ε_1 = percent strain corresponding to the cycle's lowest strain value,
P_2 = observed maximum force for the cycle (lb),
P_1 = minimum tensile load at the end of the cycle (lb), and
W_s = specimen width (ft).

The equivalent force per unit width is calculated for the last 10 cycles of each cyclic load step and averaged together to determine a single cyclic tensile modulus for each load step. The Propex Geotex 801 material was not tested because it has low strength at small stains and would not yield a representative cyclic tensile modulus. The results from the cyclic tensile modulus tests conducted by WTI are summarized in Figure 2 and Figure 3. Representative load-displacement results in the machine and cross-machine directions are shown for each geosynthetic in Appendix B.

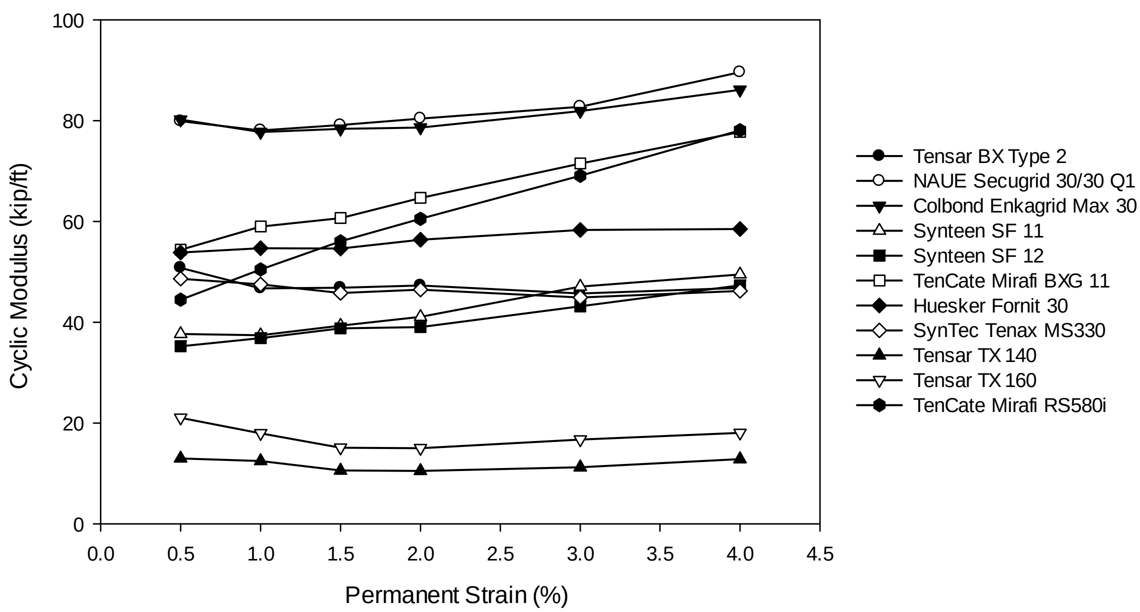

Figure 2: Cyclic tensile modulus summary - machine direction.

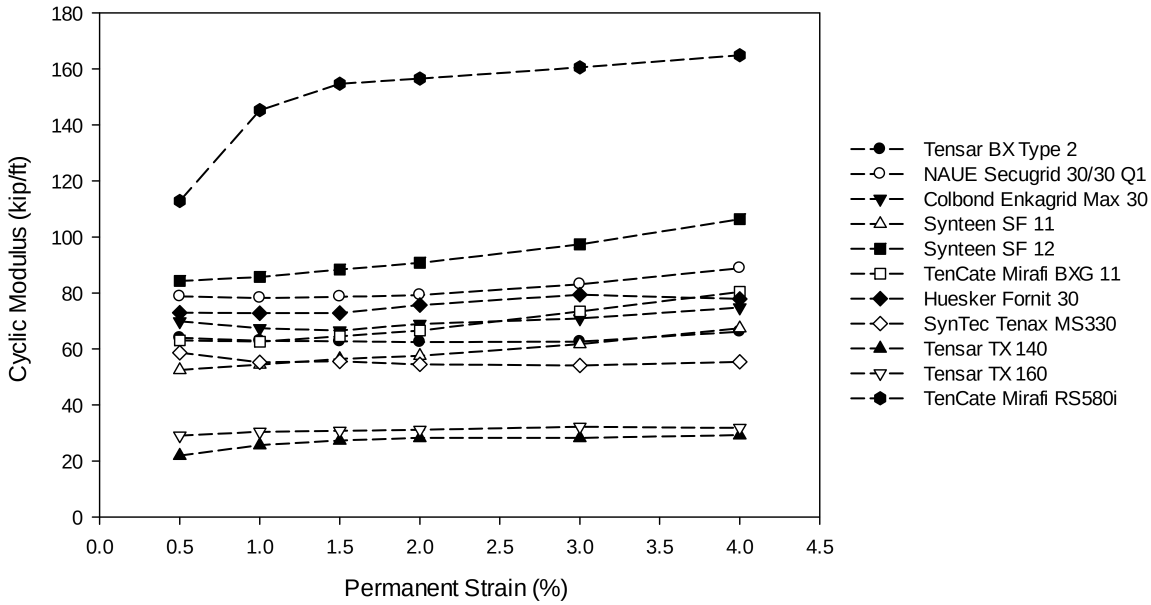

Figure 3: Cyclic tensile modulus summary - cross-machine direction.

Resilient Interface Shear Stiffness

The resilient interface shear stiffness test (ASTM D7499) is used to measure the stiffness of the interface between the geosynthetic and the surrounding soil under small cyclic loads. The test is conducted by embedding a short sample of geosynthetic in soil and applying cyclic loads at various levels of confinement and load. Applied load and displacement along the front and rear of the embedded sample are recorded. An annotated illustration of the testing device is shown in Figure 4.

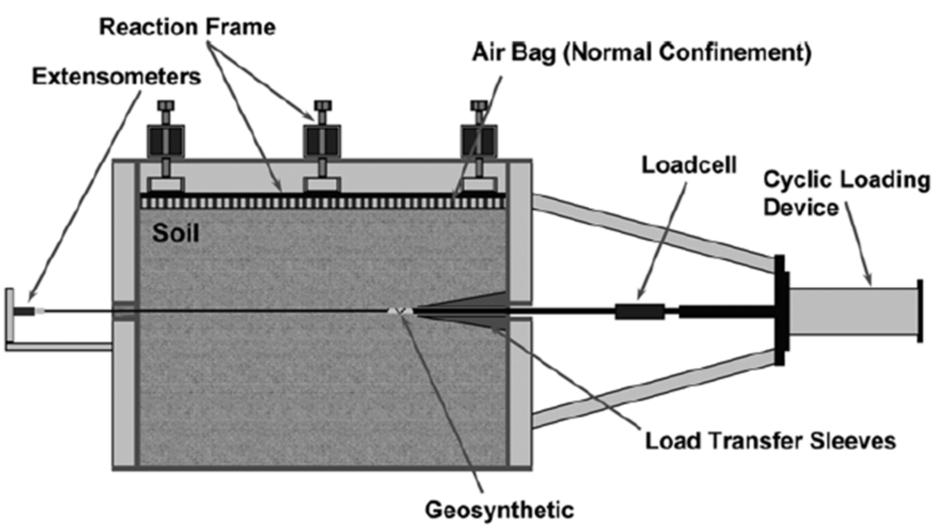

Figure 4: Resilient interface shear stiffness apparatus (from ASTM D7499).

The length of the embedded geosynthetic is specified to be 2–4 inches long and contain at least two full grid apertures; the width should be at least 12 inches. The sample length is relatively short when compared to traditional pullout tests to ensure that strain and shear stress along the length of the geosynthetic are generally uniform when loaded.

A total of six prescribed levels of horizontal cyclic force are applied to the geosynthetic at five specified levels of normal stress confinement. Resilient interface shear stiffness (G_I) is calculated from the last 10 cycles and averaged to yield a value for each step using the illustration in Figure 5, which relates the shear along the geosynthetic as it is displaced. Up to 30 values of G_I can be obtained from each test using this method (corresponding to the various levels of applied load and confinement). A regression equation based on the general equation that describes the resilient modulus of unbound granular soils (Equation 3), can be used to predict G_I. A single value for the interface normal stress (σ_I = 5.076 psi) and the interface shear stress (τ_I = 0.725 psi) were used in this analysis, based on the work conducted by Perkins and Christopher (2010). Using these estimates will facilitate relative comparisons between products. A summary of the k_1, k_2, and k_3 material parameters and G_I is provided in Table 2. Individual plots of the measured versus predicted shear modulus plots are provided in Appendix C for each of the materials.

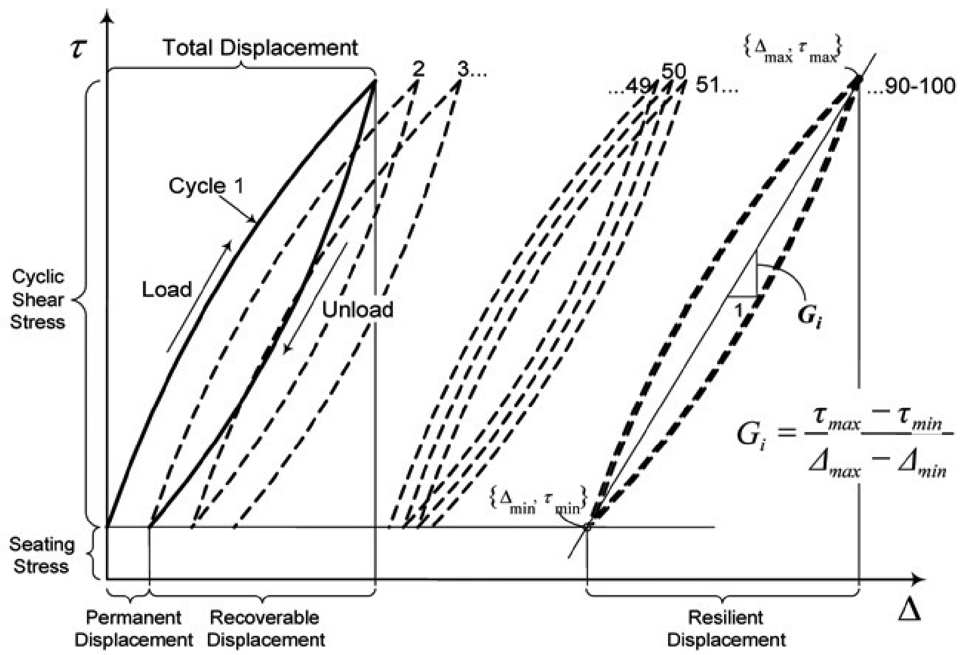

Figure 5: Illustrated calculation of resilient interface shear stiffness (from ASTM D7499).

$$G_I = k_1 P_a \left(\frac{\sigma_I}{p_a}\right)^{k_2} \left(\frac{\tau_I}{p_a} + 1\right)^{k_3} \quad \text{Equation 3}$$

where,

G_I = resilient interface shear stiffness (psi/in),
p_a = atmospheric pressure (14.69 psi),
P_a = atmospheric pressure divided by a unit length of 1 in (14.69 lb/in^3),
σ_I = interface normal stress (psi),
τ_I = interface shear stress (psi), and
k_1, k_2, and k_3 are material parameters determined from the test results.

Table 2: Summary of Resilient Interface Shear Stiffness Test Results

Geosynthetic Test Section	k_1	k_2	k_3	G_I (ksi)[a]
Tensar BX Type 2	84,611	0.92	-8.9	305
NAUE Secugrid 30/30 Q1	62,815	0.82	-15.2	186
Colbond Enkagrid Max 30	156,570	1.18	-41.0	91
Synteen SF 11	173,469	1.52	-21.7	178
Synteen SF 12	104,984	1.14	-9.4	292
TenCate Mirafi BXG 11	108,376	1.21	-12.6	240
Huesker Fornit 30	44,194	0.94	-12.9	129
SynTec Tenax MS330[b]	100,343	1.17	-16.8	190
Tensar TX 140	44,176	0.62	-27.8	88
Tensar TX 160	103,015	1.12	-13.4	242
TenCate Mirafi RS580i	59,303	0.81	-2.3	329
Propex Geotex 801	46,413	0.88	-12.4	147

[a] Interface normal stress σ_I = 5.076 psi and Interface shear stress τ_I = 0.725 psi used for all calculations
[b] Tested as a composite (i.e., all three layers of geosynthetic together)

Junction Strength

Junction strength tests (ASTM D7737) on the geogrids were conducted by SGI Testing Services (Norcross, GA) in the cross-machine direction only. These tests are used to verify that the junctions of a particular geogrid have sufficient strength to undergo construction stresses, but may also potentially provide a way to quantify how well the grid structure transfers loads from members orthogonal to the direction of the applied load. The junction strength tests generally involve specimens to be cut in the shape of a "T" with at least one transverse member protruding from either side of the junction being tested. The specimen is gripped on both sides of the "T" and the orthogonal rib is pulled until failure of the junction occurs. A typical junction strength test setup is shown in Figure 6**.** Test data for these tests is summarized in Table 3 for the tests conducted by SGI as well as values published by the manufacturers. Plots of the junction strength with respect to displacement are shown for each material in Appendix D.

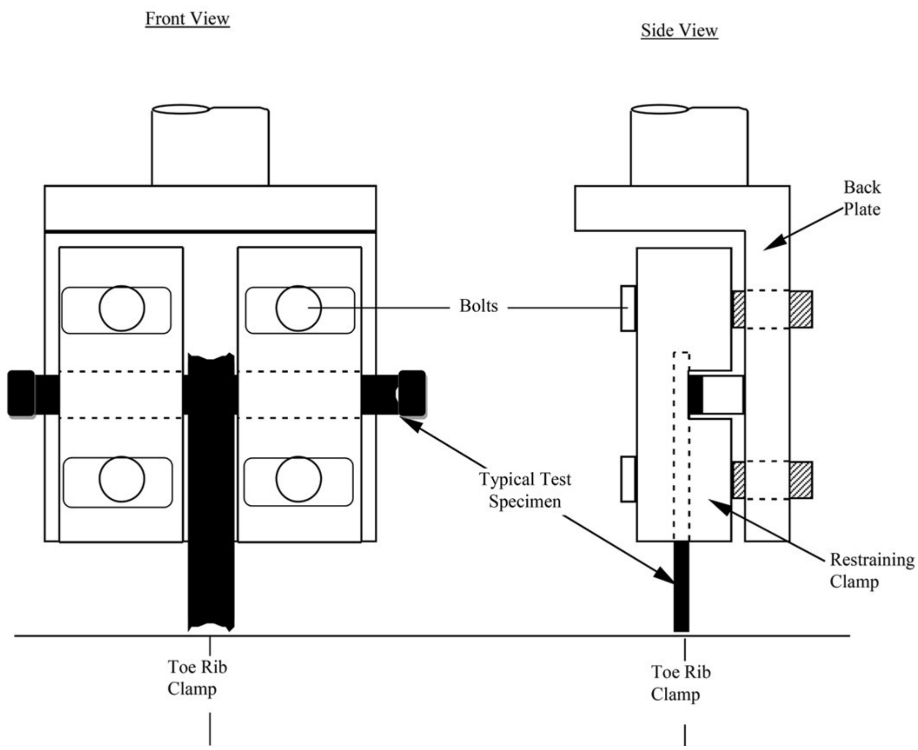

Figure 6: Typical junction strength test specimen setup. (from ASTM D7737)

Table 3: Summary of Junction Strength Test Results

Geosynthetic Test Section	Tested by SGI				Published by Manufacturer			
	Strength (lb/junction)		Strength (lb/in)		Strength (lb/junction)		Strength (lb/in)	
	MD	XMD	MD	XMD	MD	XMD	MD	XMD
Tensar BX Type 2	NT	206.7	NT	171.6	NP	NP	NP	NP
NAUE Secugrid 30/30 Q1	NT	90.6	NT	57.6	80.4[a]	80.9[a]	51.4	51.4
Colbond Enkagrid Max 30	NT	106.6	NT	49.5	NP	NP	NP	NP
Synteen SF 11	NT	46.1	NT	37.1	59.4	47.6	47.9[b]	38.3[b]
Synteen SF 12	NT	34.4	NT	28.6	59.4	64.8	48.4[b]	53.8[b]
TenCate Mirafi BXG 11	NT	42.5	NT	35.8	NP	NP	NP	NP
Huesker Fornit 30	NT	8.9	NT	10.5	NP	NP	NP	NP
SynTec Tenax MS330	NT	310.8[c]	NT	196.6[c]	206.1[a]	259.6[a]	106.2	164.2
Tensar TX 140	NT	111.8	NT	72.4	NP		NP	
Tensar TX 160	NT	123.4	NT	75.1	NP		NP	
TenCate Mirafi RS580i	NA		NA		NA		NA	
Propex Geotex 801	NA		NA		NA		NA	

[a] Values published by the manufacturer were in lb/ft. WTI adjusted these values to determine lb/junction
[b] Values published by the manufacturer were in lb/junction. WTI adjusted these values to determine junction strength in lb/in.
[c] Tested a single layer and multiplied by 3 (three layer material)
NA = Not Applicable
NP = Information was not provided by the manufacturer
NT = Not Tested

Aperture Stability Modulus

Aperture stability modulus tests were performed by SGI based on the method developed by Kinney (2000). The test is used to quantify the dimensional stiffness of a geogrid under a torsional load. Similar to the junction strength tests, the aperture stability tests can only be performed on geosynthetics that have open apertures (i.e., geogrids). The test is conducted by confining a square sample of geogrid in a stiff stationary square clamp, where the interior 9" x 9" portion of the material is not clamped, as shown in Figure 7. A moment is then applied to the center of the geogrid at five load increments and the degree of rotation is measured. The aperture stability modulus (*ASM*) is defined as the torque (17.70 in-lb), divided by the rotation at that torque (see Equation 4 below). According to the draft standard, the test is stopped if the rotation reaches 20 degrees. In this case the highest torque should be used in the equation, and the report should state that the aperture stability modulus is less than the calculated value (Kinney, 2000). The results for the aperture stability modulus tests performed by SGI and published by the manufacturers are shown in Table 4. Individual plots for each material are provided in Appendix E.

$$ASM = \frac{Torque\ (17.70\ in{-}lb)}{Rotation\ (deg.)} \qquad \text{Equation 4}$$

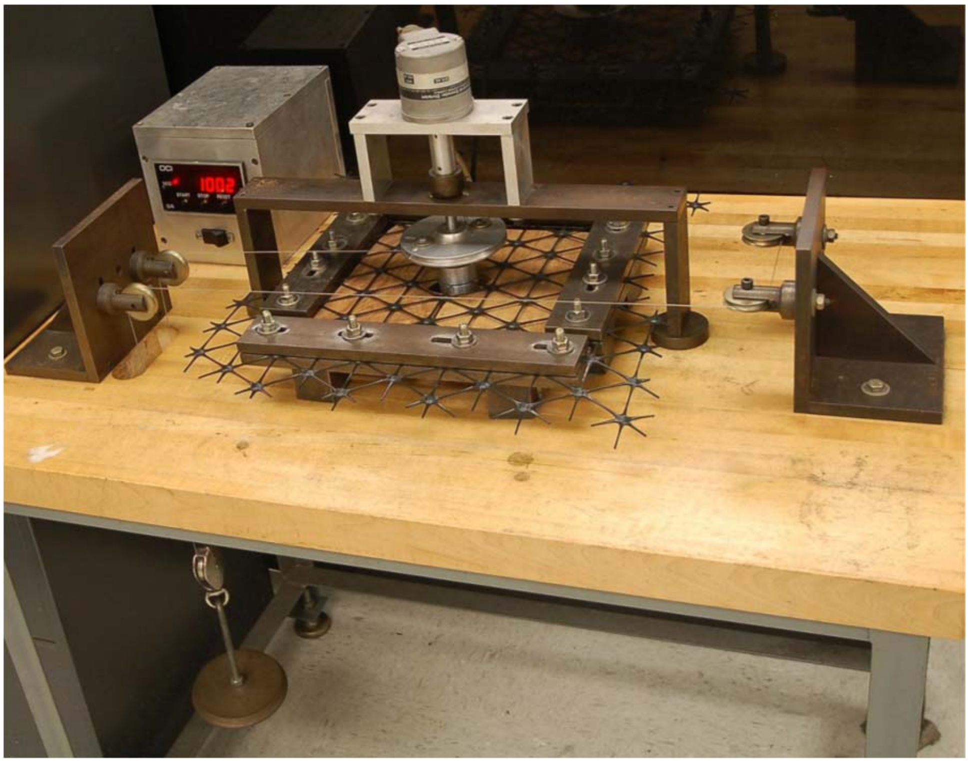

Figure 7: Aperture stability modulus testing device (photo courtesy of Tensar International, Inc.).

Table 4: Summary of Aperture Stability Modulus Test Results

Geosynthetic Test Section	Tested by SGI: Aperture Stability Modulus (in-lb/deg)	Published by Manufacturer: Aperture Stability Modulus (in-lb/deg)
Tensar BX Type 2	6.9	5.75
NAUE Secugrid 30/30 Q1	10.2	9.90
Colbond Enkagrid Max 30	13.9	NP
Synteen SF 11	2.2	NP
Synteen SF 12	2.4	NP
TenCate Mirafi BXG 11	3.1	NP
Huesker Fornit 30	9.6	6.55
SynTec Tenax MS330	3.2[a]	NP
Tensar TX 140	2.5	2.60[b]
Tensar TX 160	4.9	3.13[b]
TenCate Mirafi RS580i	NA	NA
Propex Geotex 801	NA	NA

[a] Tested a single layer, and multiplied by 3 (three layer material)
[b] Test was performed using a torque of 4.34 in-lb. (the standard is 17.70 lb-in), which may imply that the aperture stability modulus is less than the value published by the manufacturer (Kinney, 2000).
NA = Not Applicable
NP = Information was not provided by the manufacturer

References

ASTM D7499-09 (2009) *Standard Test Method for Measuring Geosynthetic-Soil Resilient Interface Shear Stiffness*, West-Conshohocken, PA, ASTM International.

ASTM D7556-10 (2010) *Standard Test Method for Determining Small-Strain Tensile Properties of Geogrids and Geotextiles by In-Air Cyclic Tension Tests*, West-Conshohocken, PA, ASTM International.

ASTM D7737-11 (2011) *Standard Test Method for Individual Geogrid Junction Strength*, West-Conshohocken, PA, ASTM International.

Cuelho, E. (1998) "Determination of Geosynthetic Constitutive Parameters and Soil/Geosynthetic Interaction by In-Air and In-Soil Experiments," Thesis submitted in partial fulfillment of the requirements for the degree of Master of Science in Civil Engineering, Montana State University – Bozeman.

Kinney, T. (2000) Standard Test Method for Determining the "Aperture Stability Modulus" of a Geogrid, Seattle, Shannon & Wilson, Inc.

Perkins, S. and Christopher, B. (2010) "Development of Design Charts for Unpaved Road Using NAUE Geosynthetics: Phases I, II & III," Final report to NAUE GmbH & Co. KG.

Appendix A–Wide-Width Tensile Strength Load-Displacement Plots

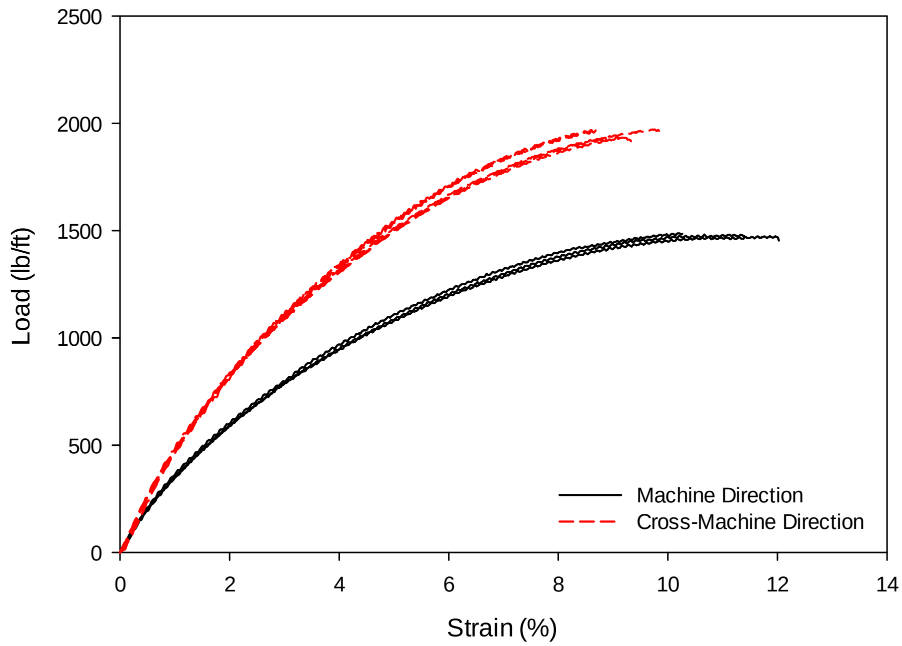

Figure A-1: Tensar BX Type 2.

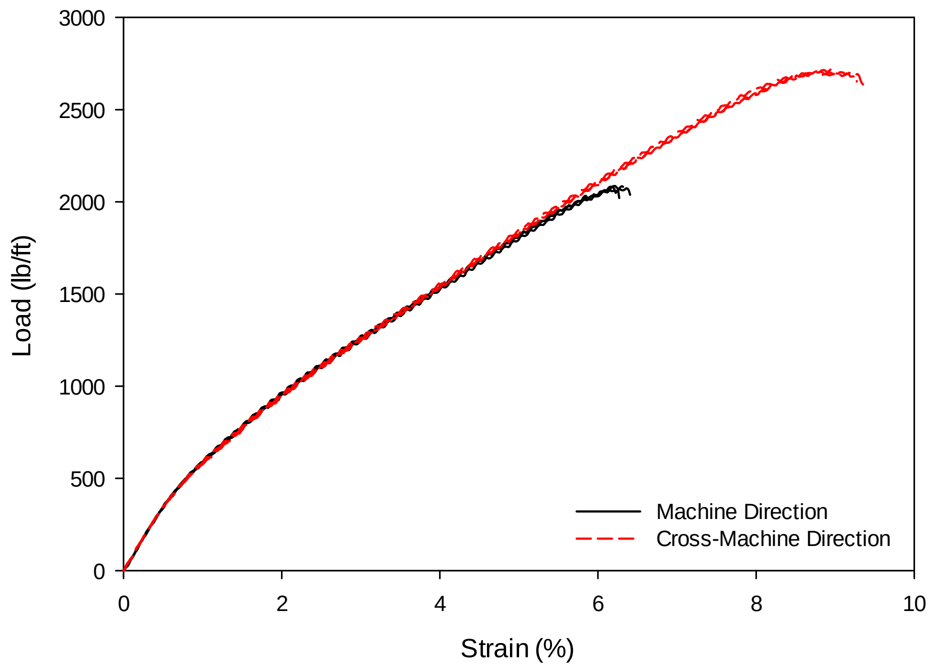

Figure A-2: NAUE Secugrid 30/30 Q1.

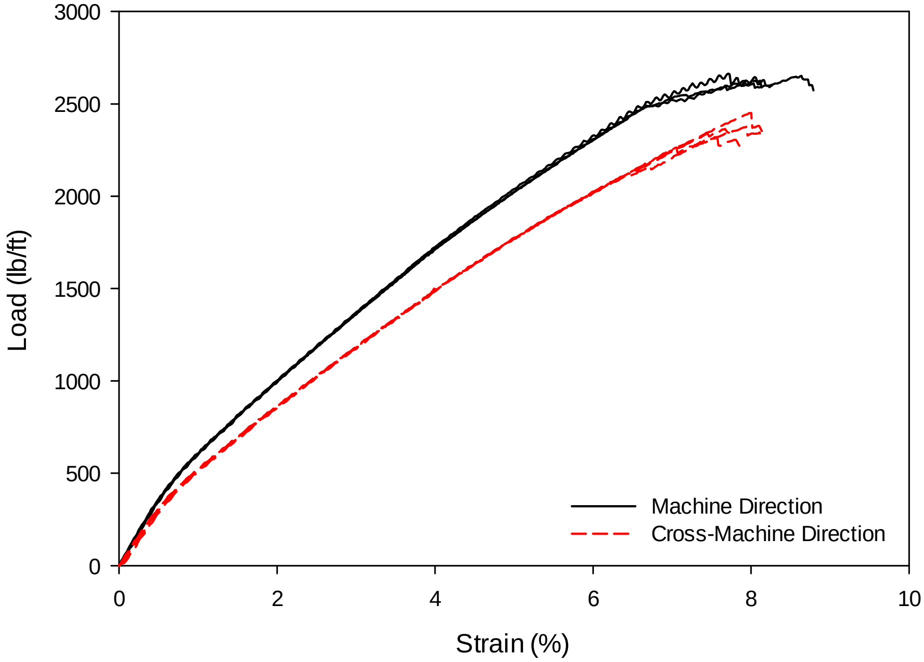

Figure A-3: Colbond Enkagrid Max 30.

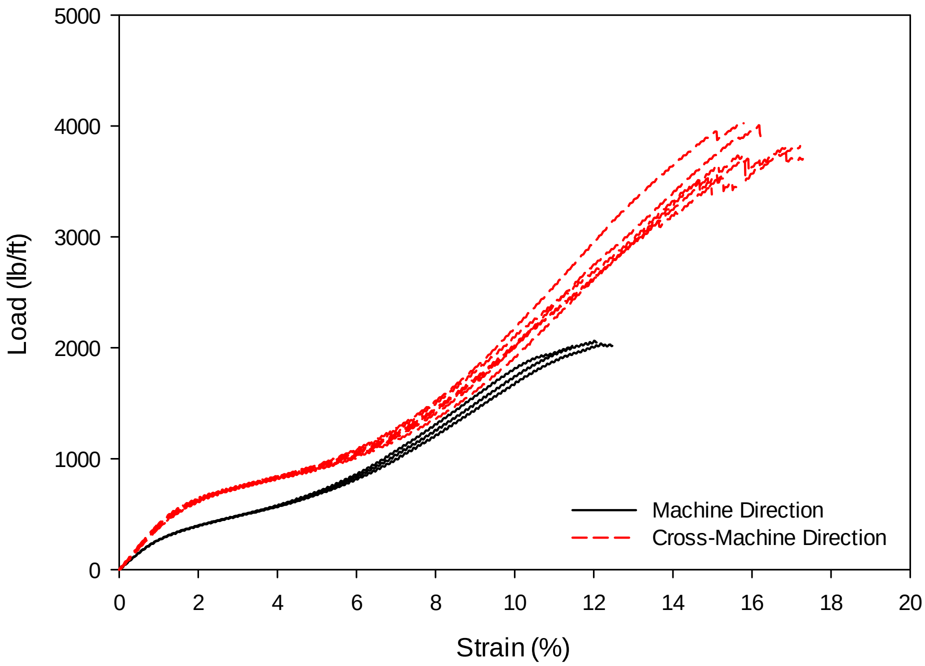

Figure A-4: Synteen SF-11.

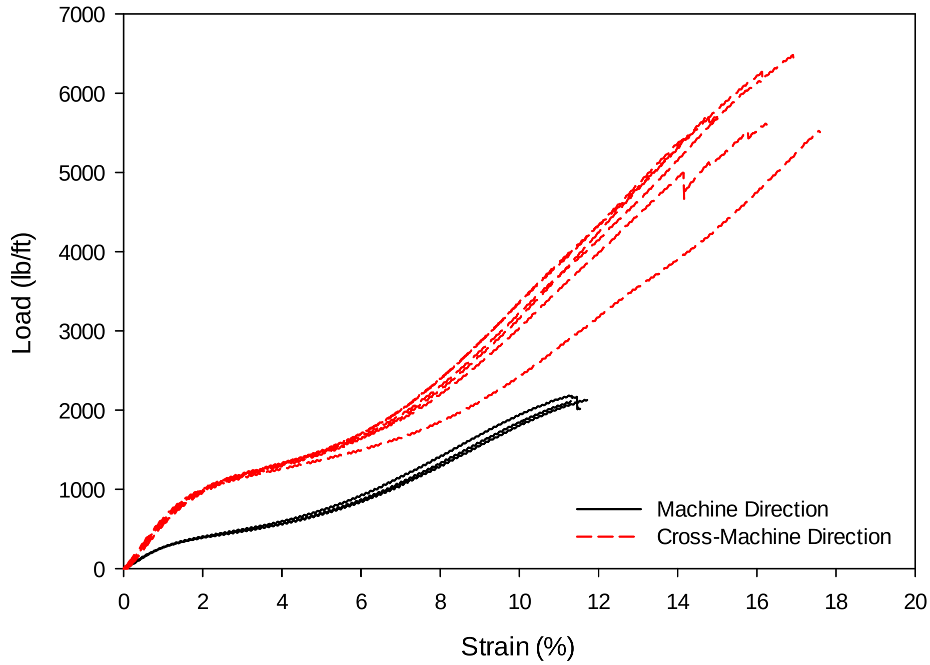

Figure A-5: Synteen SF-12.

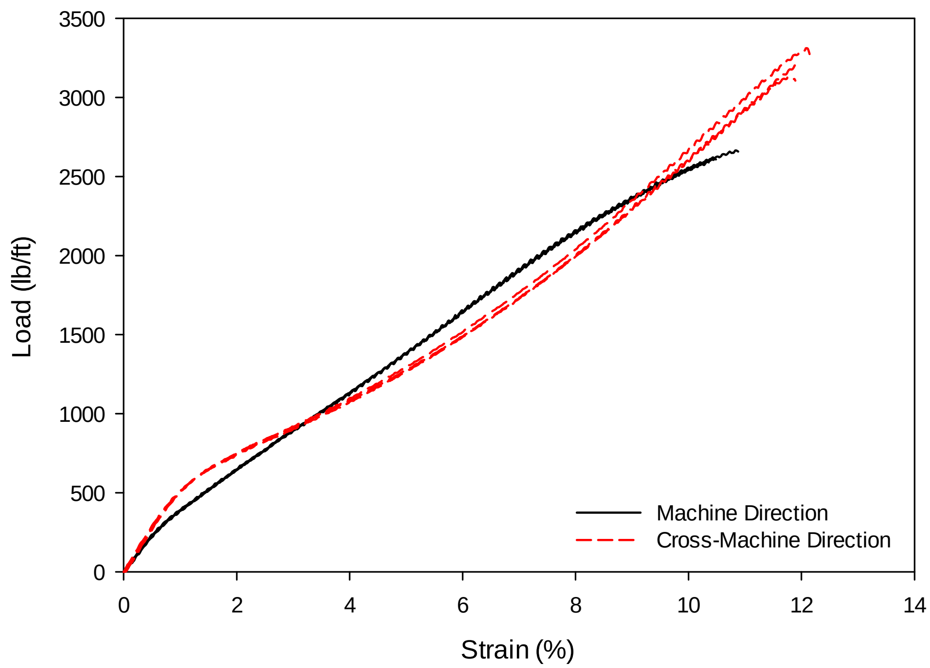

Figure A-6: TenCate Mirafi BXG-11.

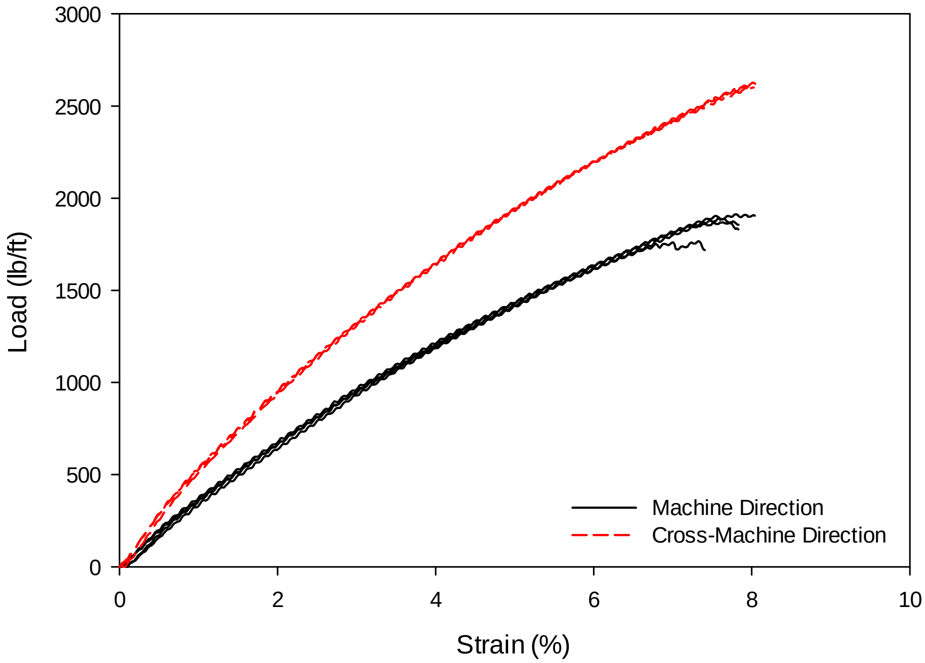

Figure A-7: Huesker Fornit 30.

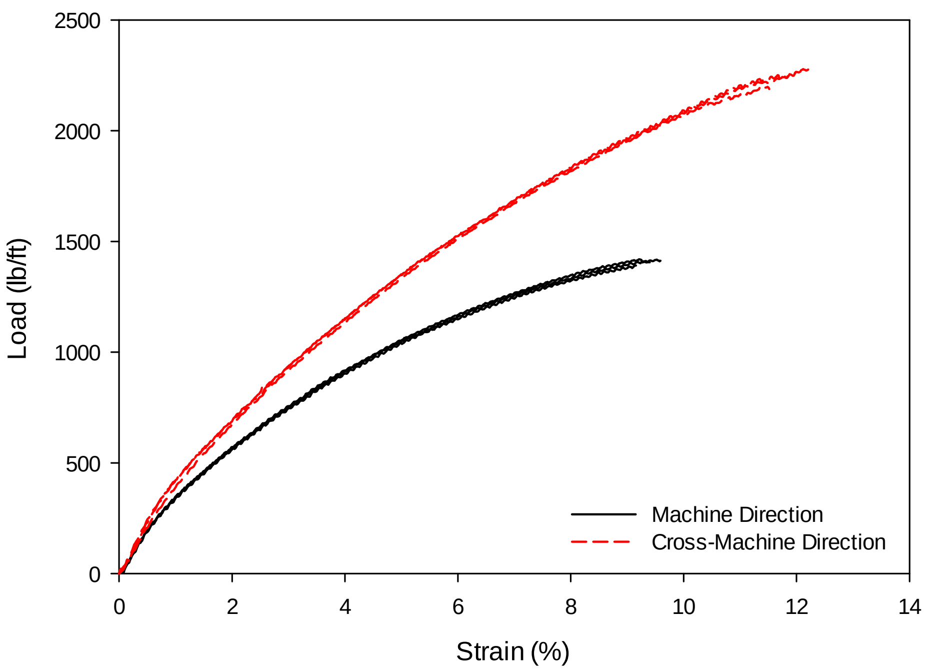

Figure A-8: SynTec Tenax MS330.

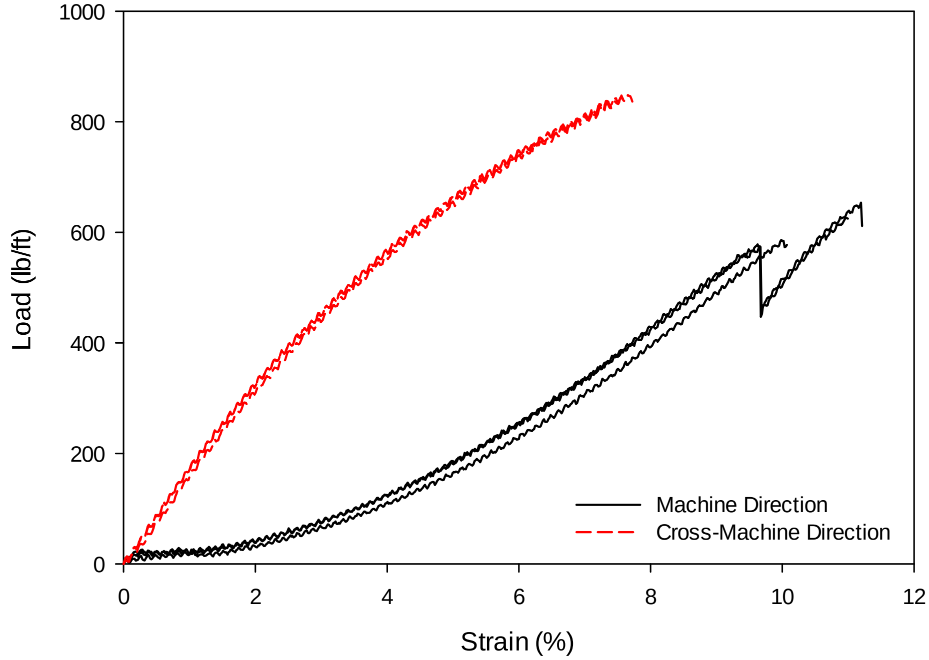

Figure A-9: Tensar TX 140.

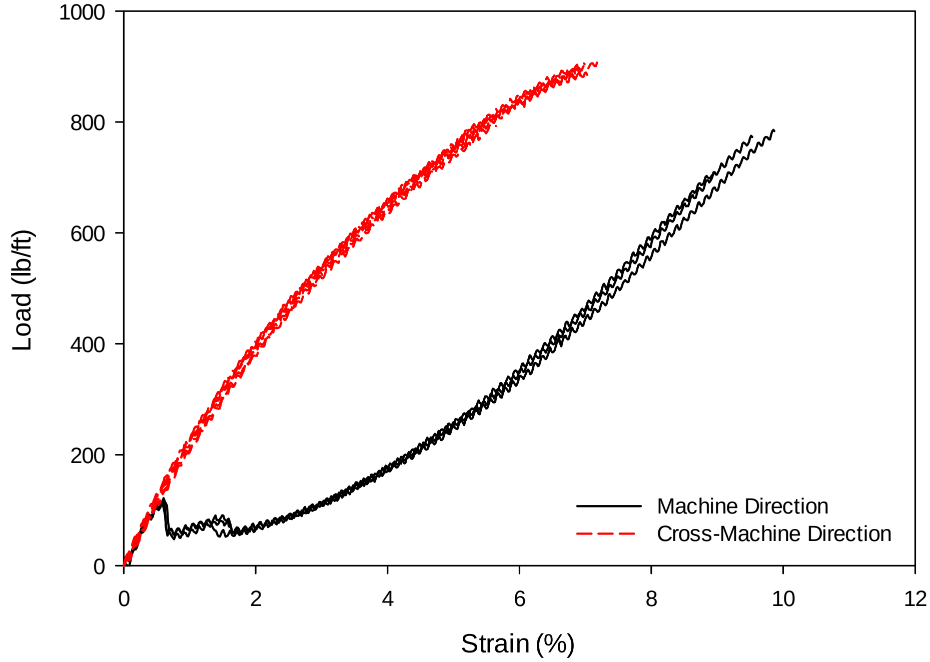

Figure A-10: Tensar TX-160.

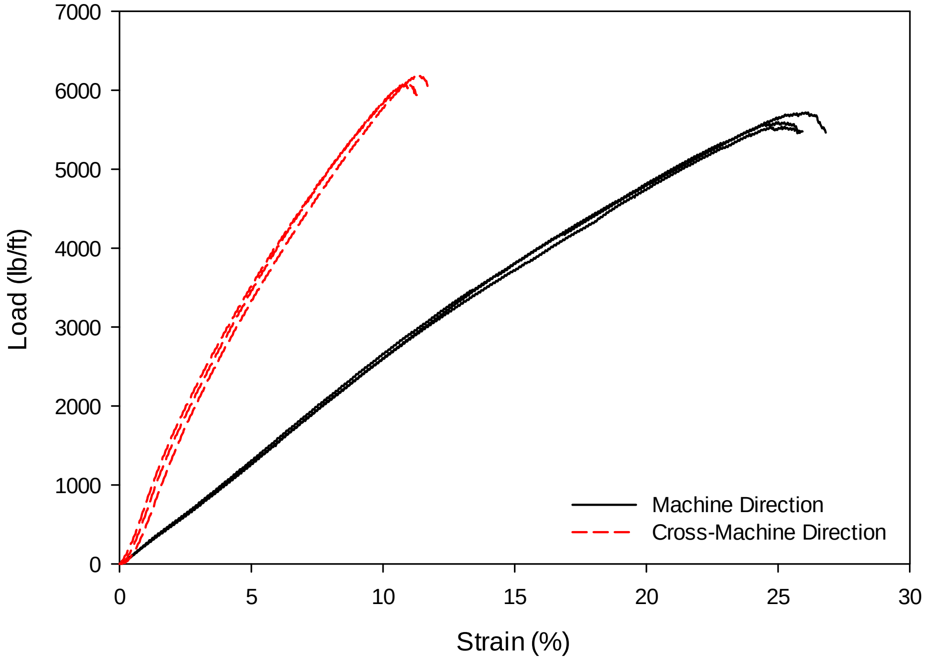

Figure A-11: TenCate Mirafi RS580i.

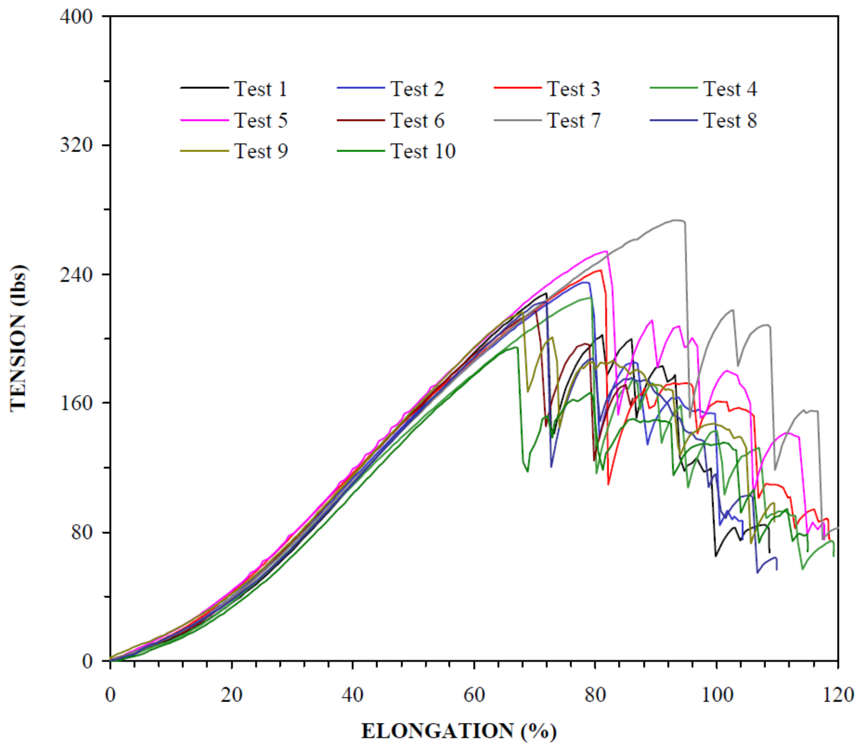

Figure A-12: Propex Geotex 801 (grab strength - machine direction)

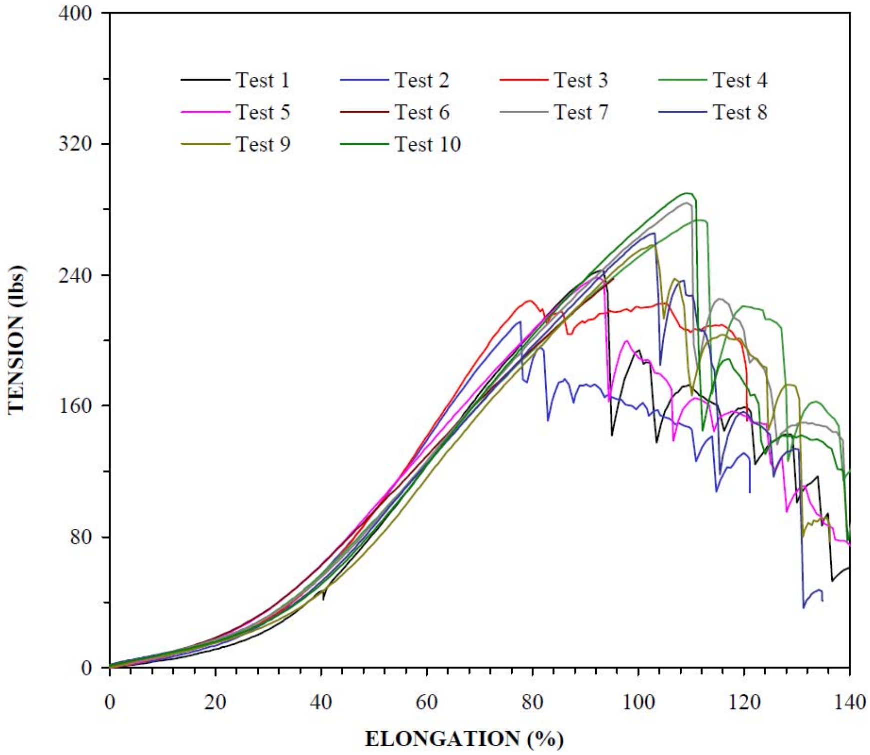

Figure A-13: Propex Geotex 801 (grab strength - cross-machine direction)

Appendix B–Cyclic Tensile Modulus Load-Displacement Plots

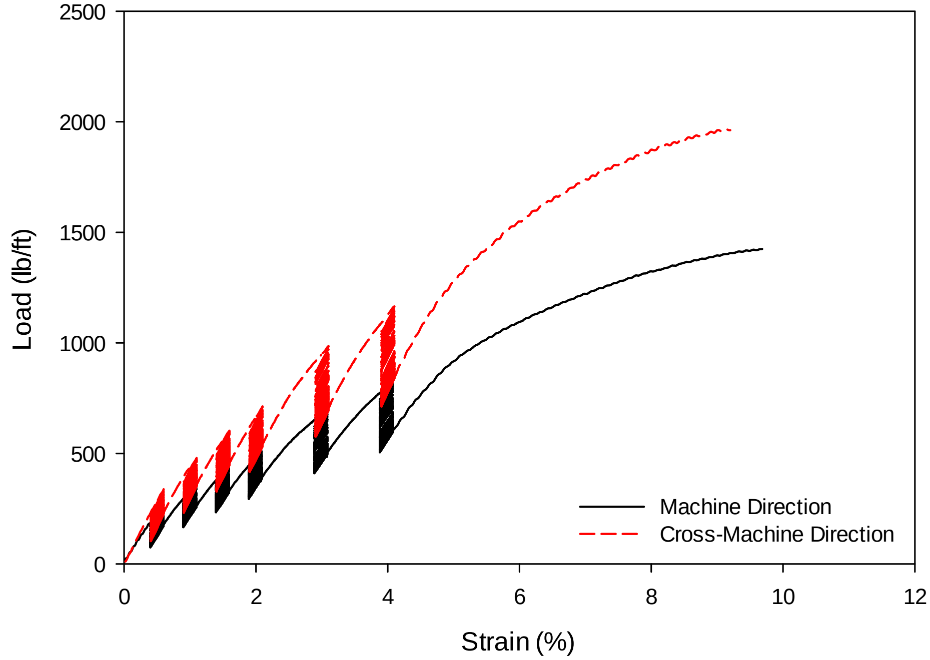

Figure B-1: Tensar BX Type 2.

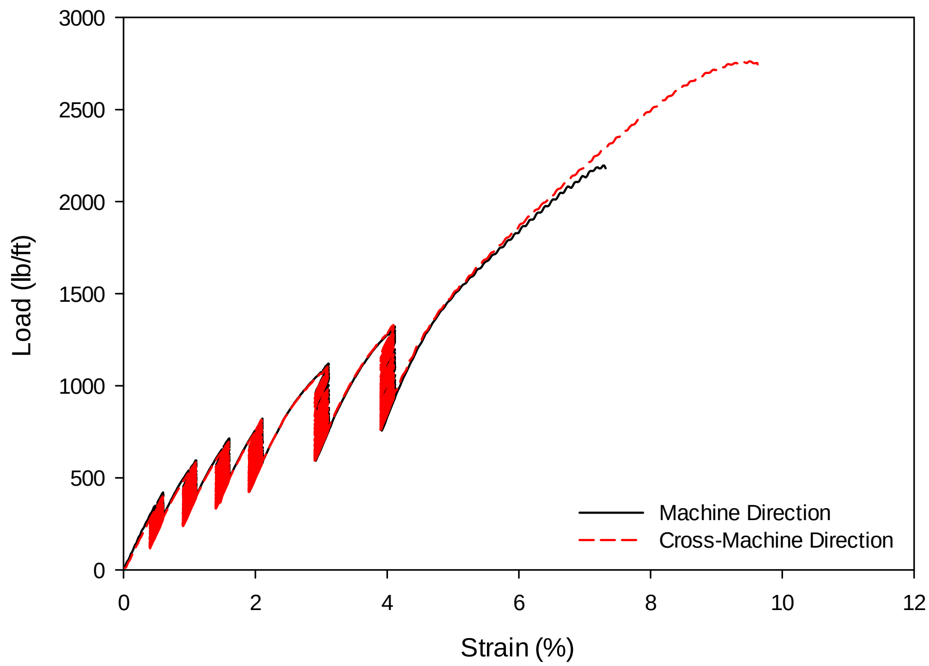

Figure B-2: NAUE Secugrid 30/30 Q1.

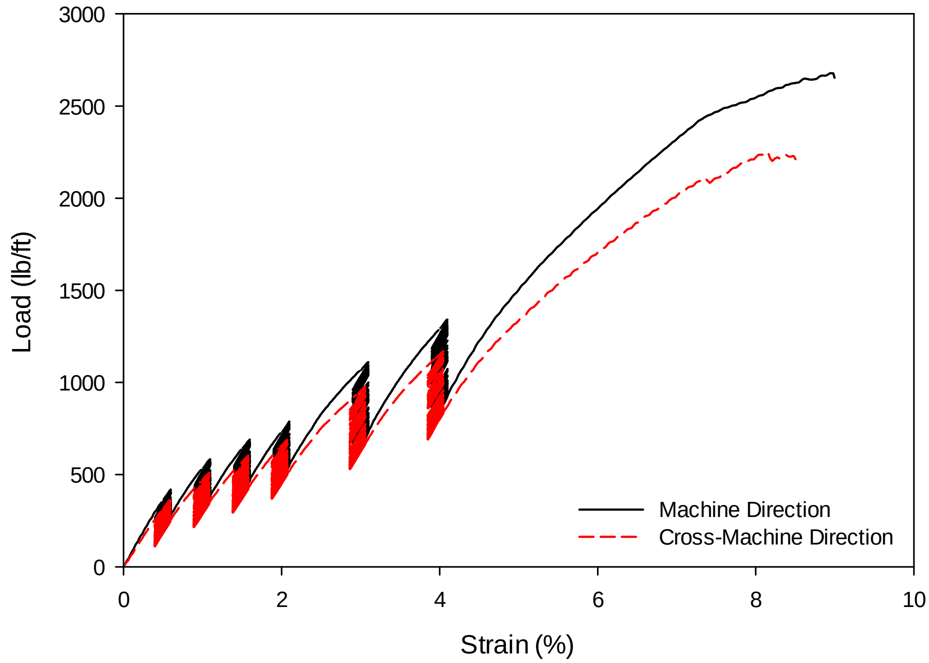

Figure B-3: Colbond Enkagrid Max 30.

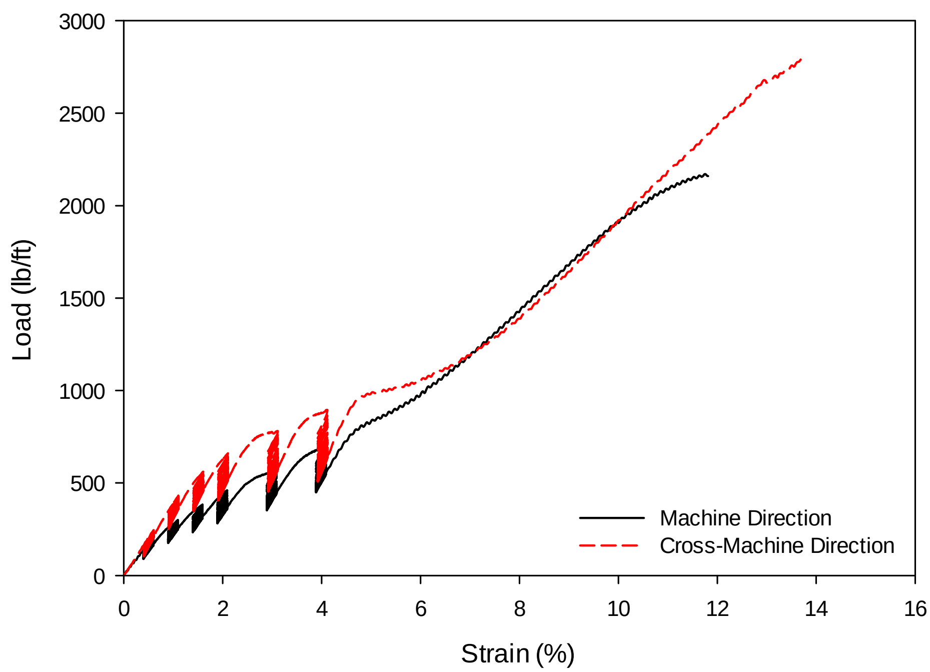

Figure B-4: Synteen SF 11.

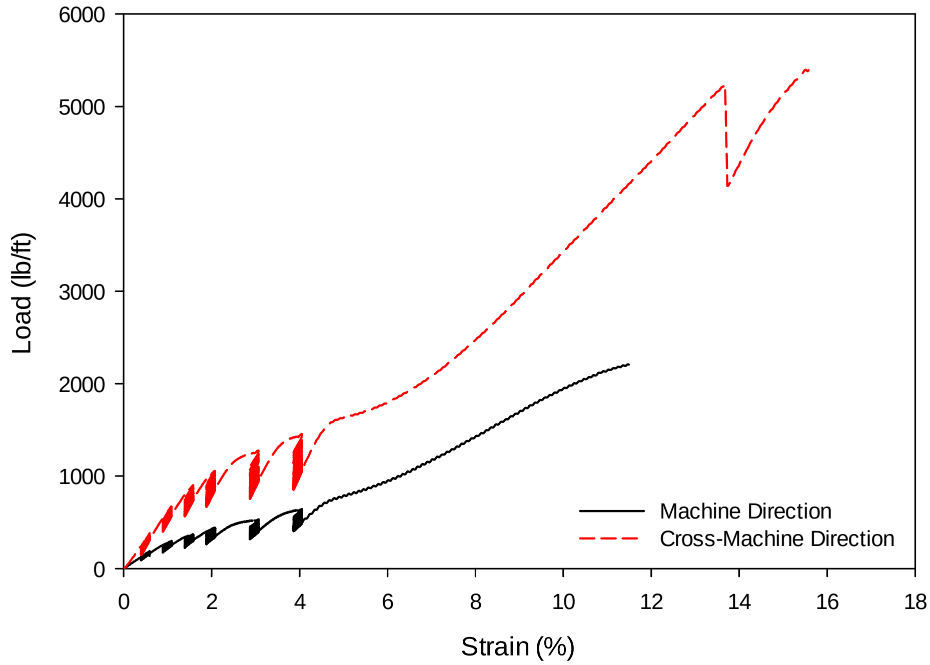

Figure B-5: Synteen SF 12.

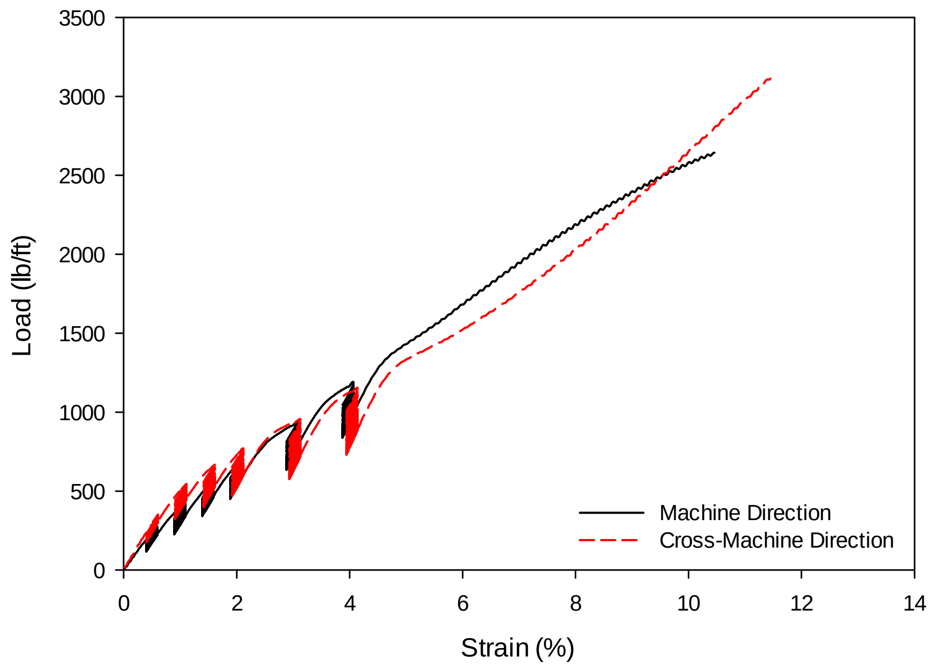

Figure B-6: TenCate Mirafi BXG 11.

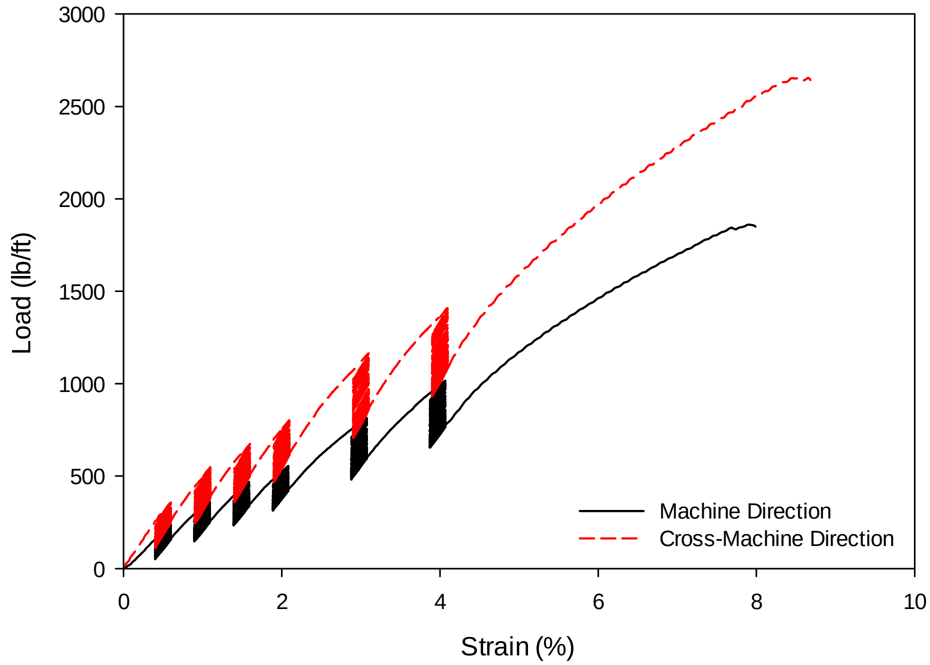

Figure B-7: Huesker Fornit 30.

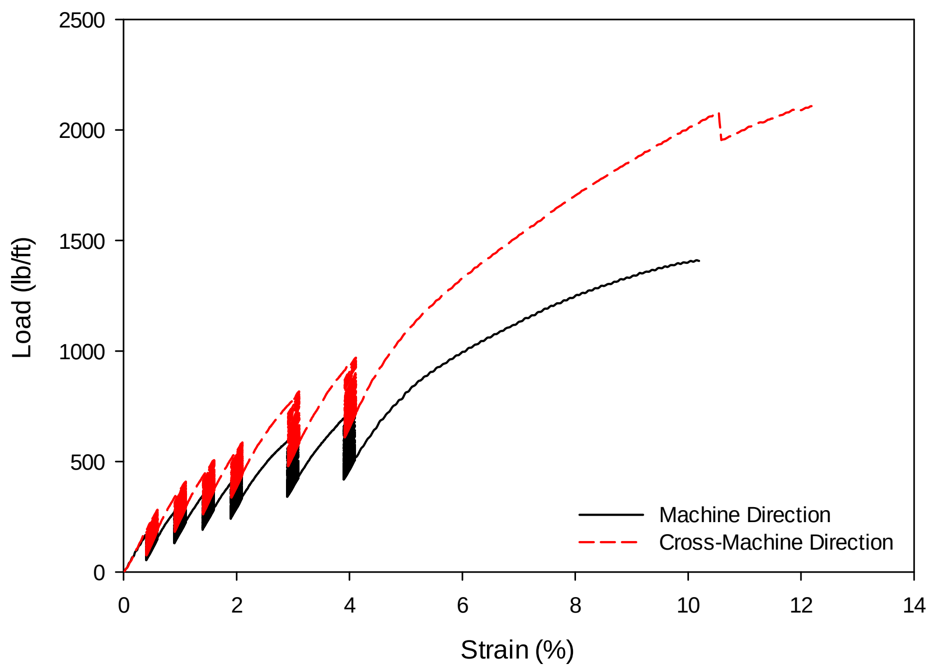

Figure B-8: SynTec Tenax MS330.

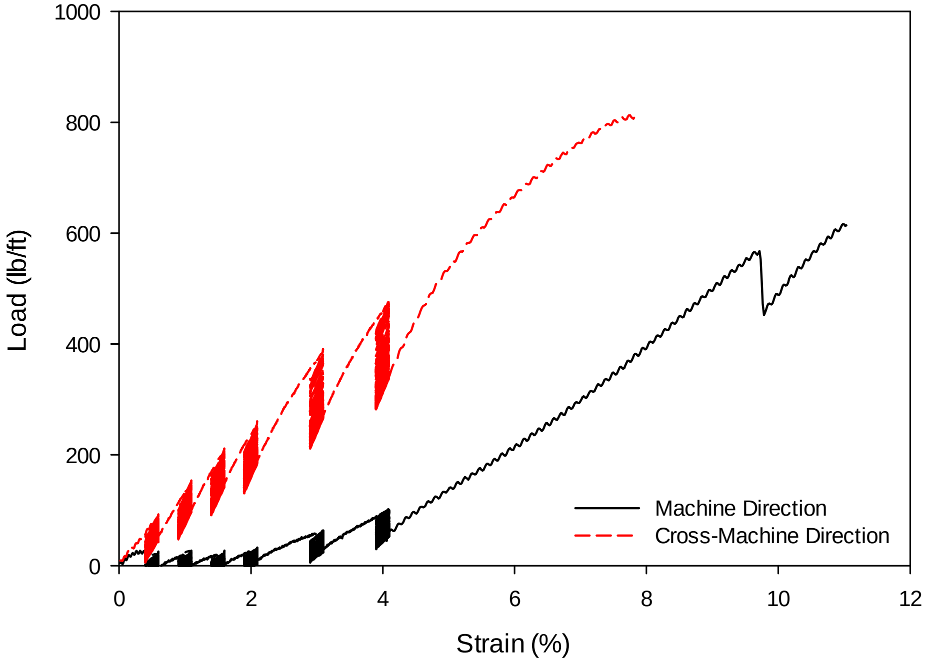

Figure B-9: Tensar TX 140.

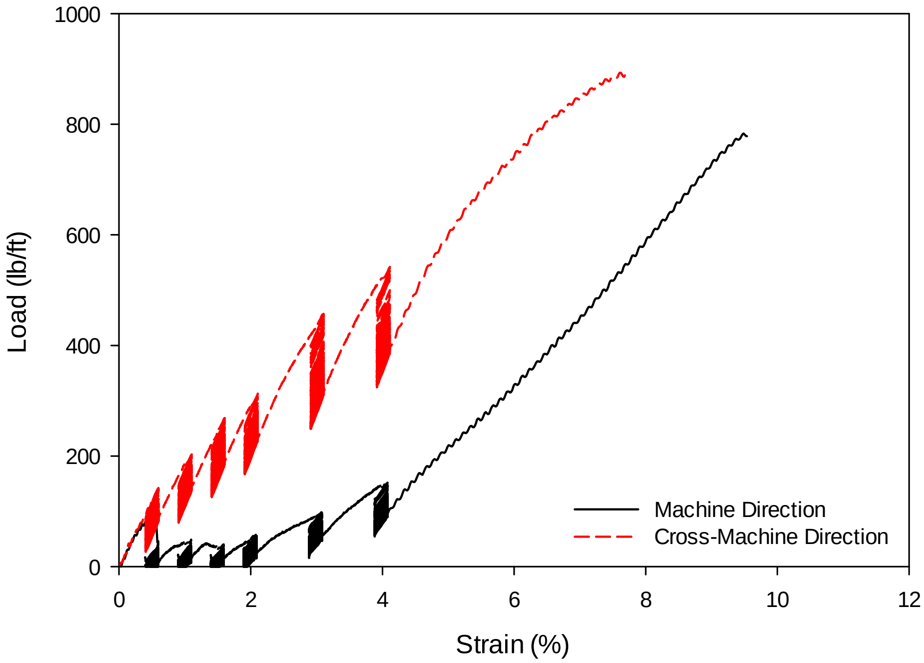

Figure B-10: Tensar TX 160.

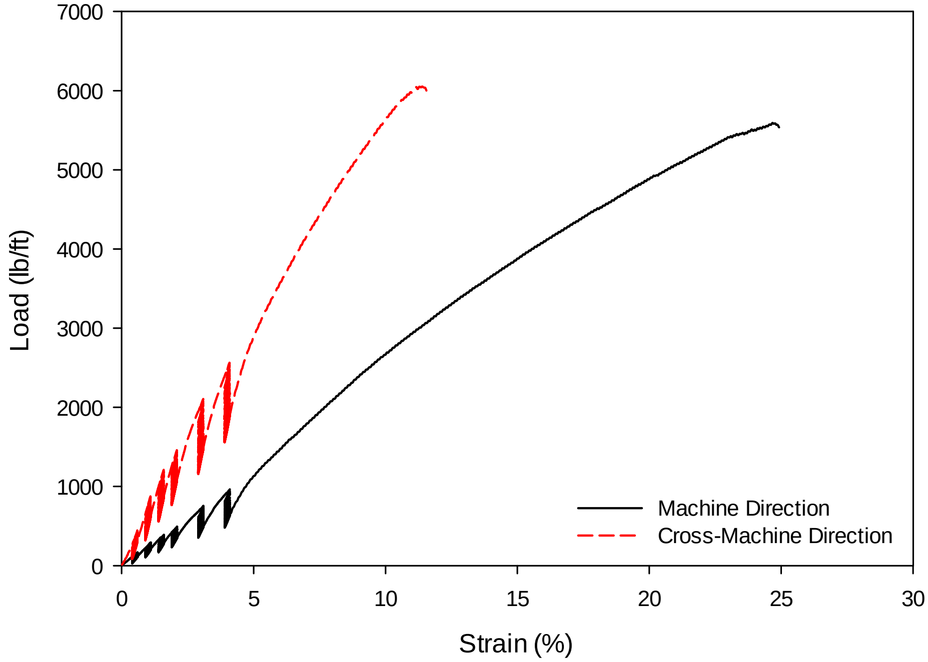

Figure B-11: TenCate Mirafi RS580i.

Appendix C–Resilient Interface Shear Stress Plots

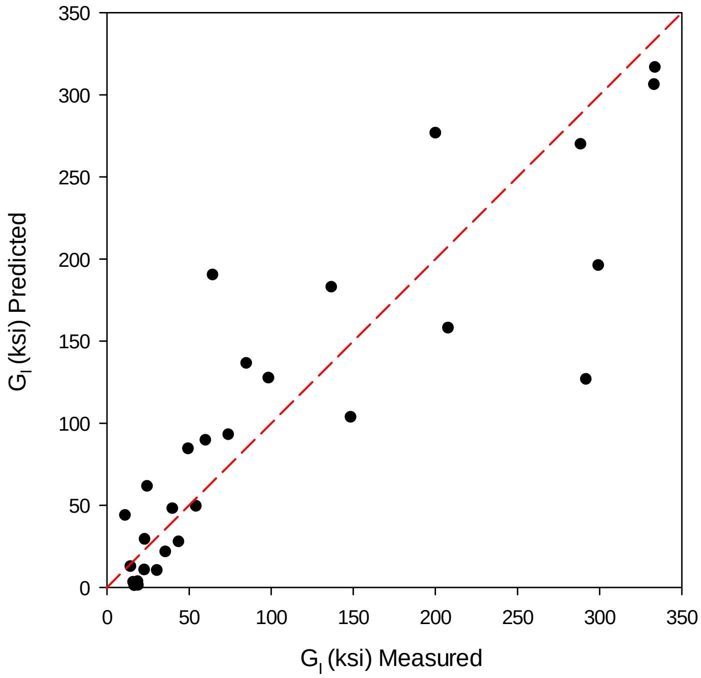

Figure C-1: Tensar BX Type 2.

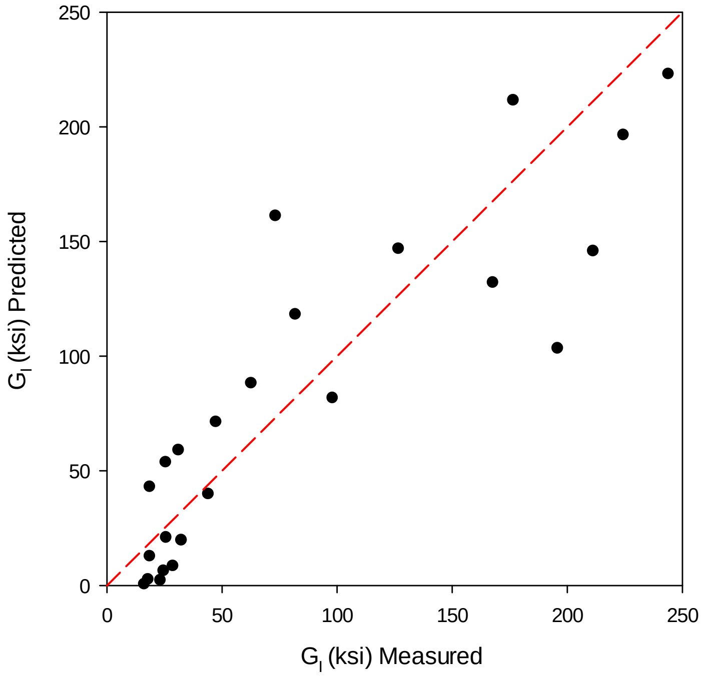

Figure C-2: NAUE Secugrid 30/30 Q1.

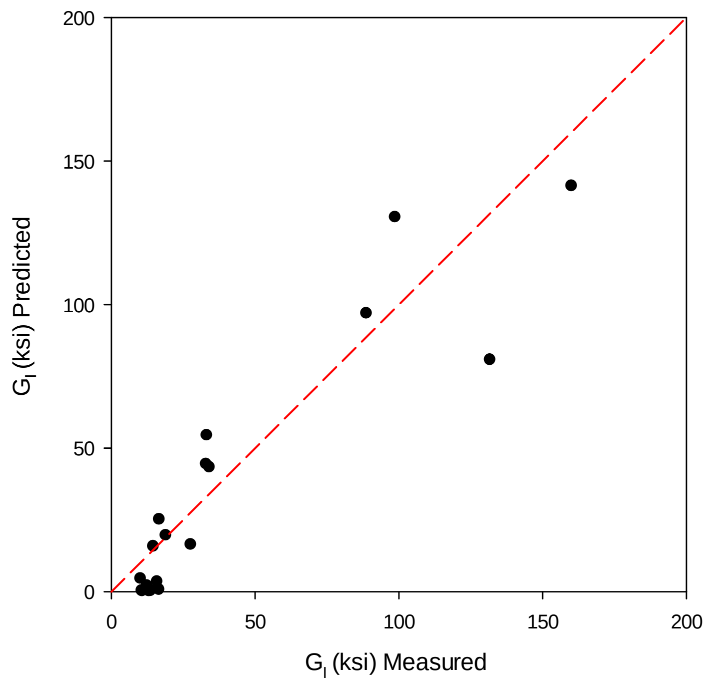

Figure C-3: Colbond Enkagrid Max 30.

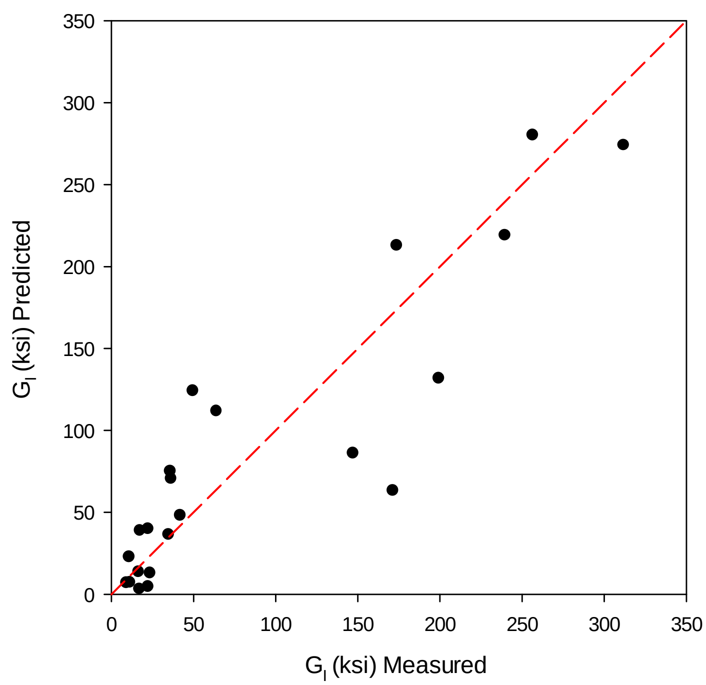

Figure C-4: Synteen SF 11.

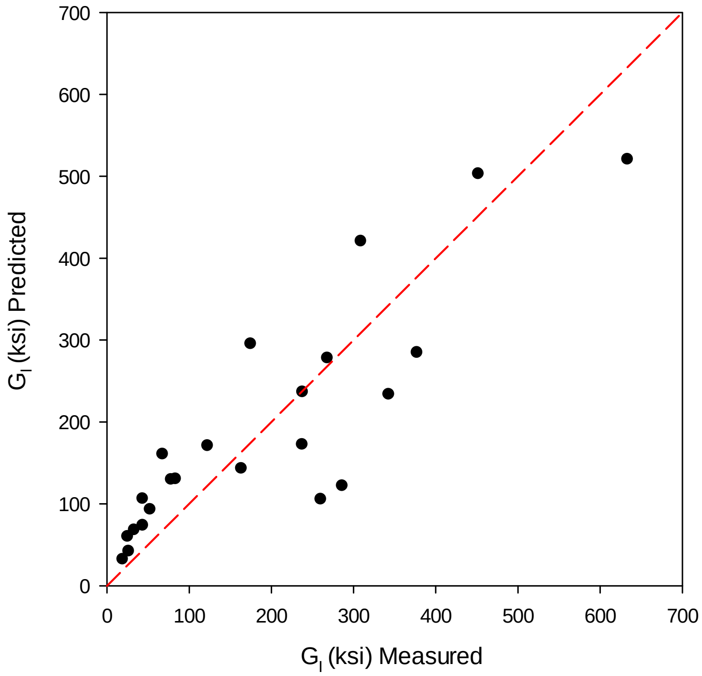

Figure C-5: Synteen SF 12.

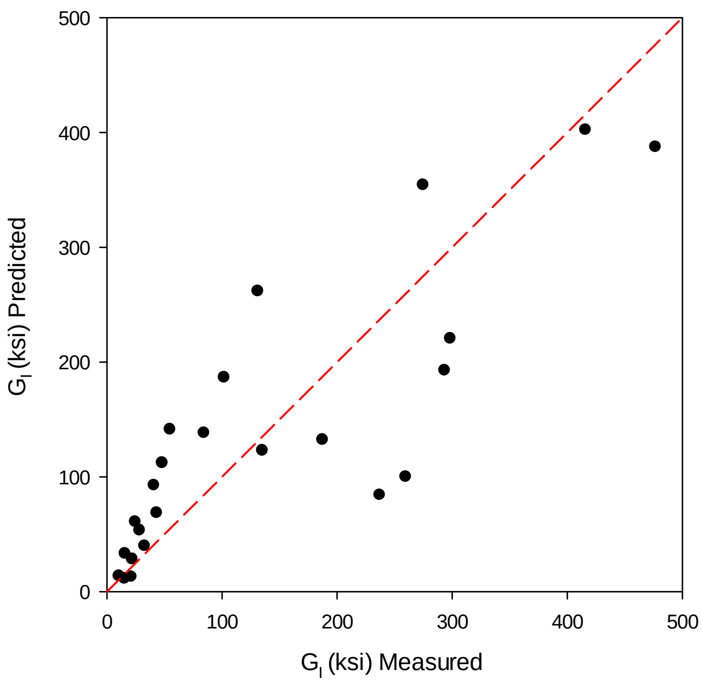

Figure C-6: TenCate Mirafi BXG 11.

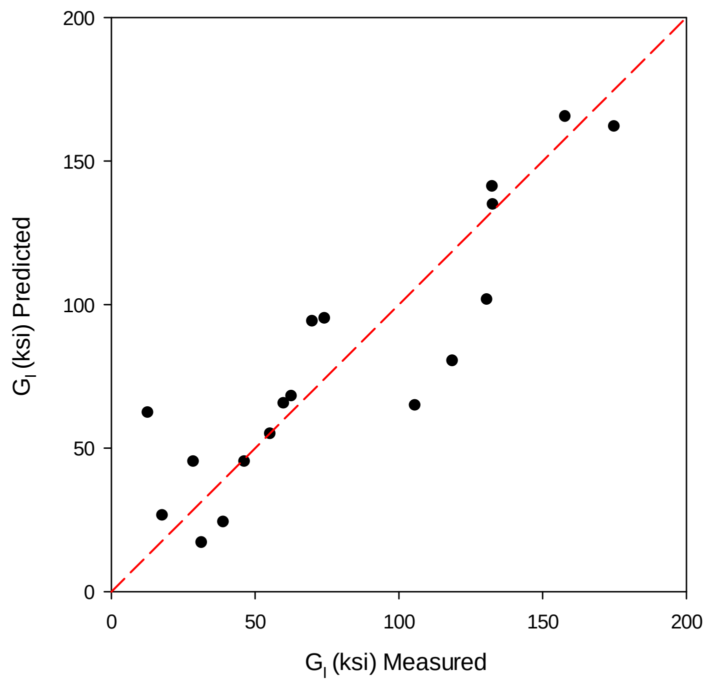

Figure C-7: Huesker Fornit 30.

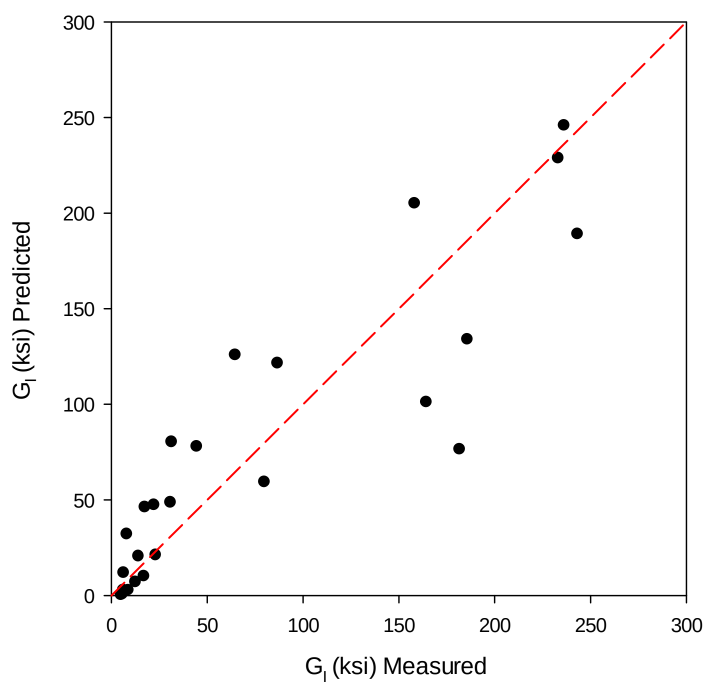

Figure C-8: SynTec Tenax MS330.

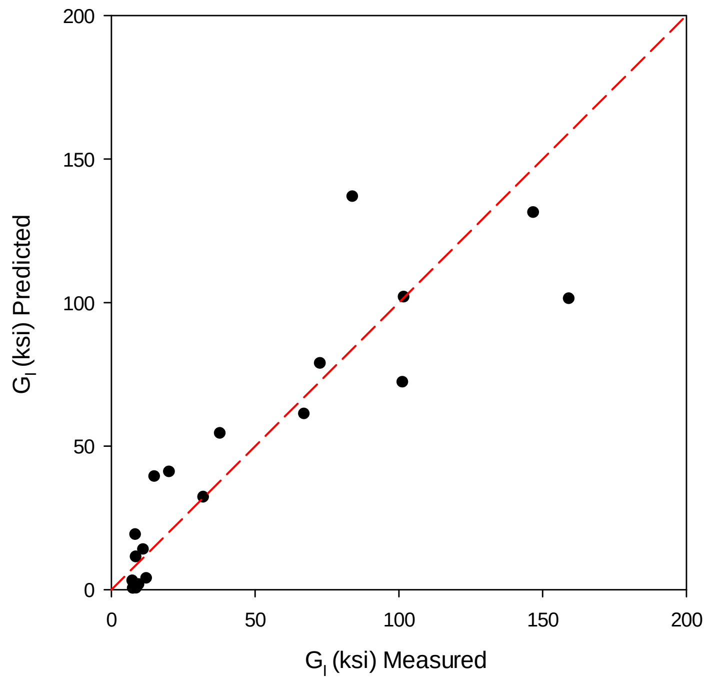

Figure C-9: Tensar TX 140.

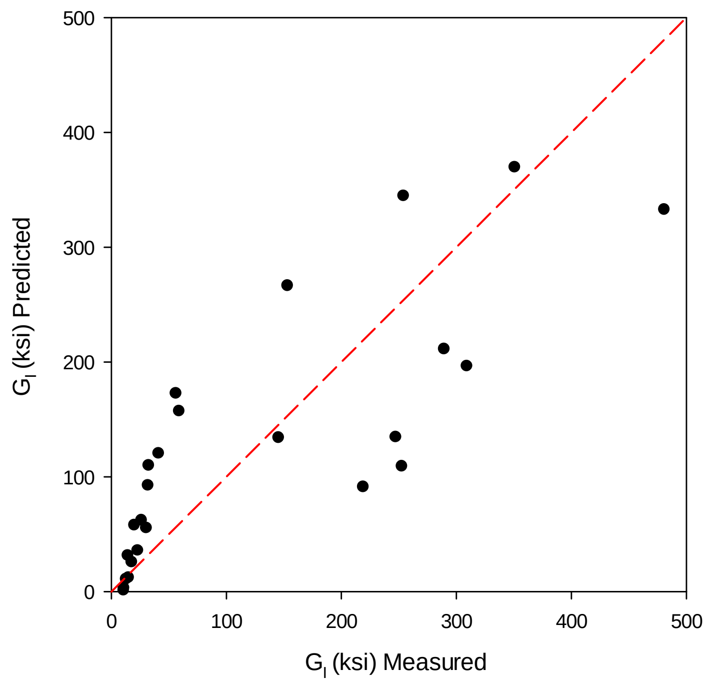

Figure C-10: Tensar TX 160.

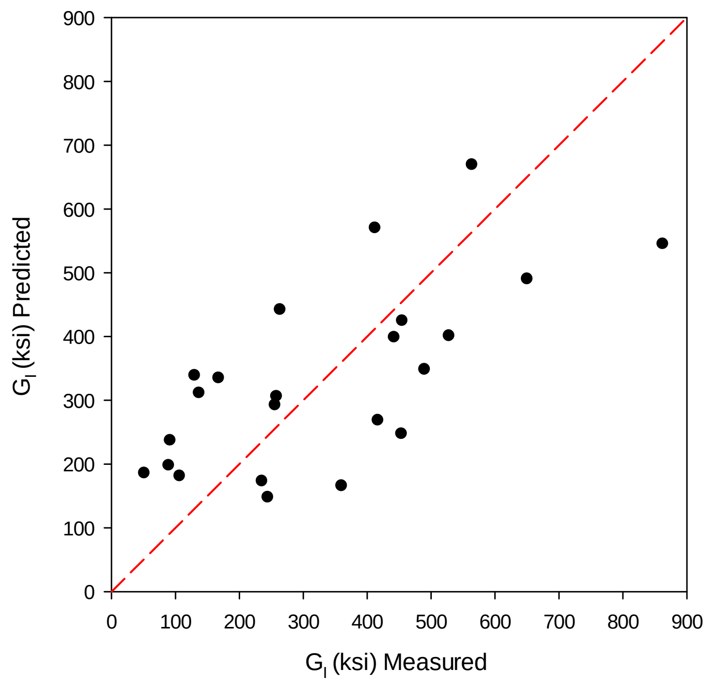

Figure C-11: TenCate Mirafi RS580i.

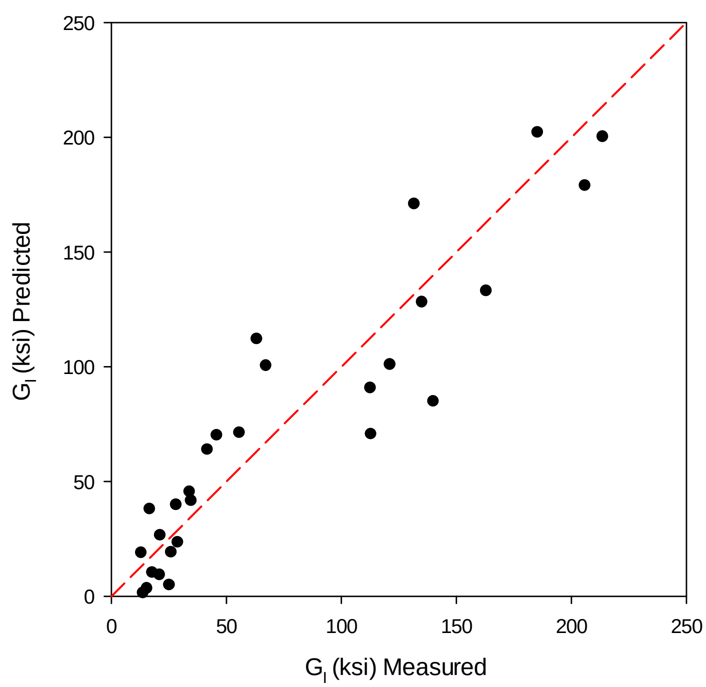

Figure C-12: Propex Geotex 801.

Appendix D–Junction Strength Load-Displacement Plots

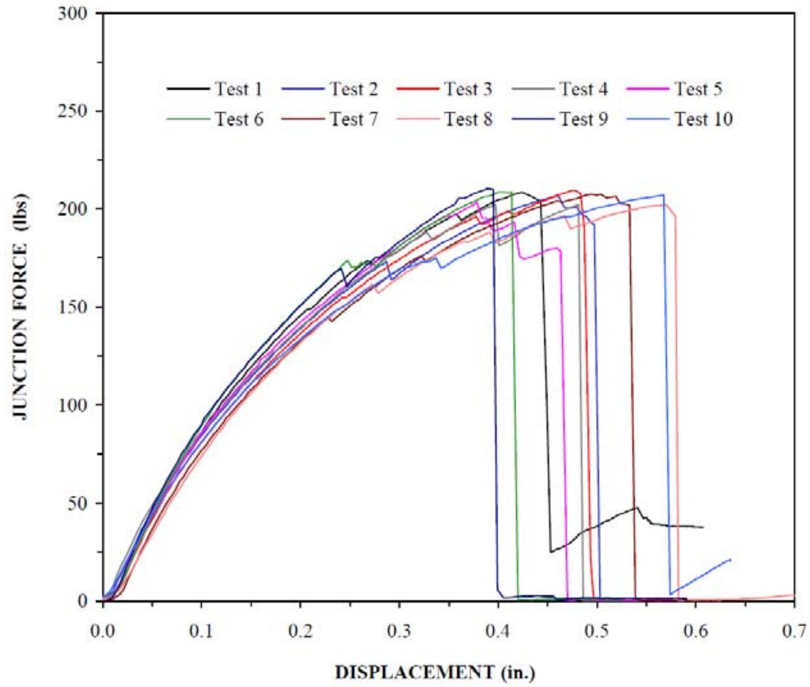

Figure D-1: Tensar BX Type 2.

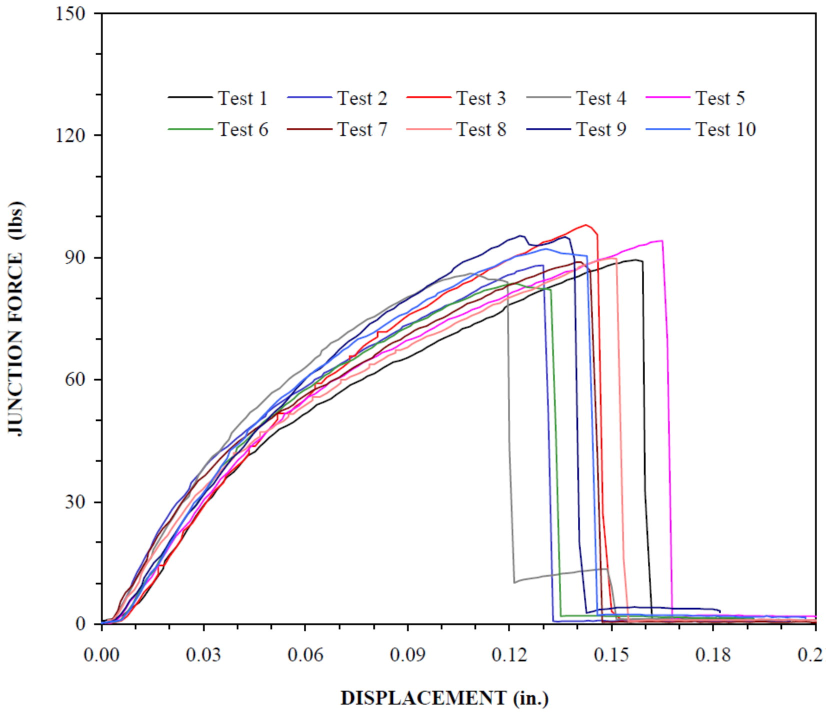

Figure D-2: NAUE Secugrid 30/30 Q1.

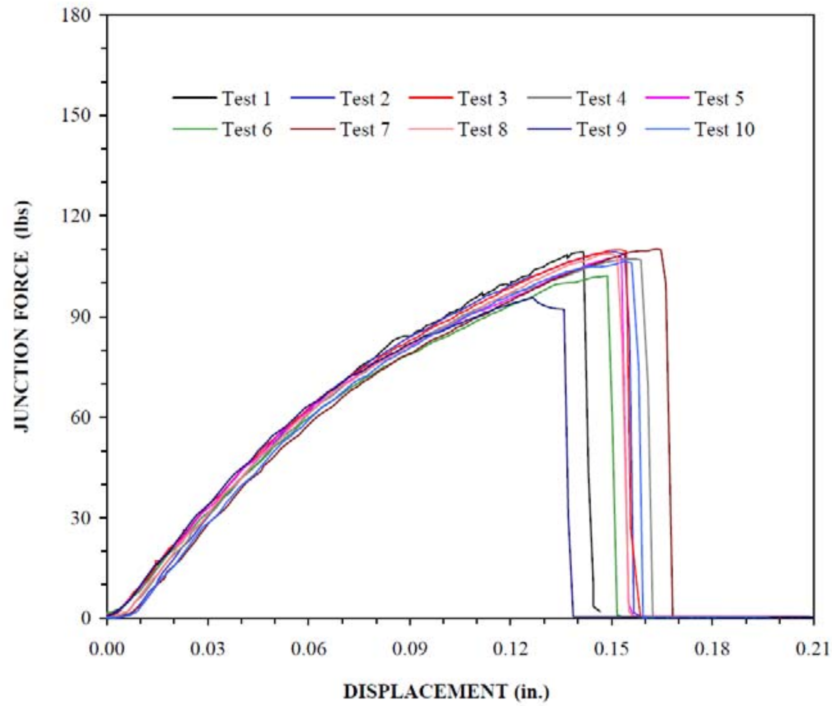

Figure D-3: Colbond Enkagrid Max 30.

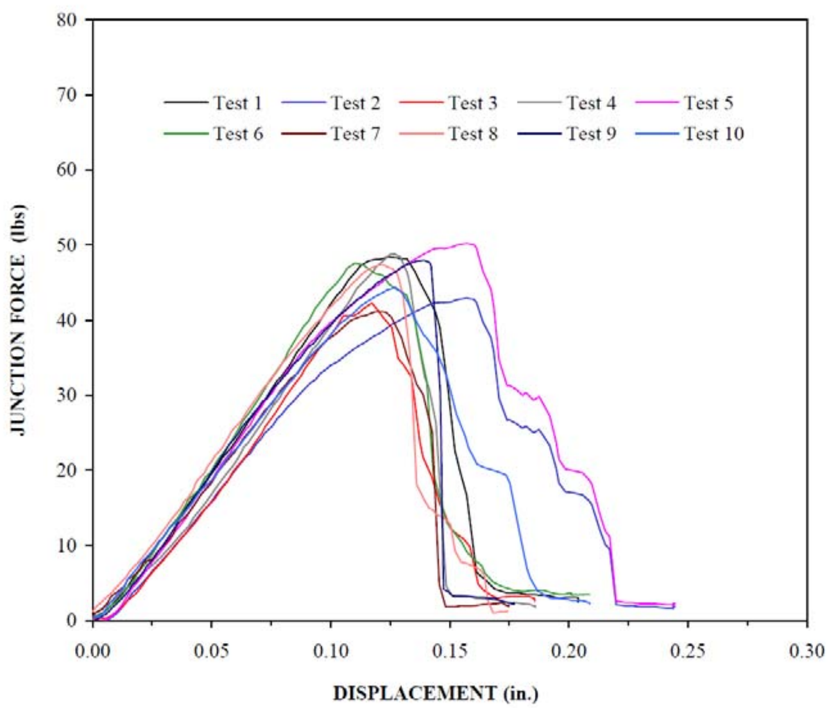

Figure D-4: Synteen SF 11.

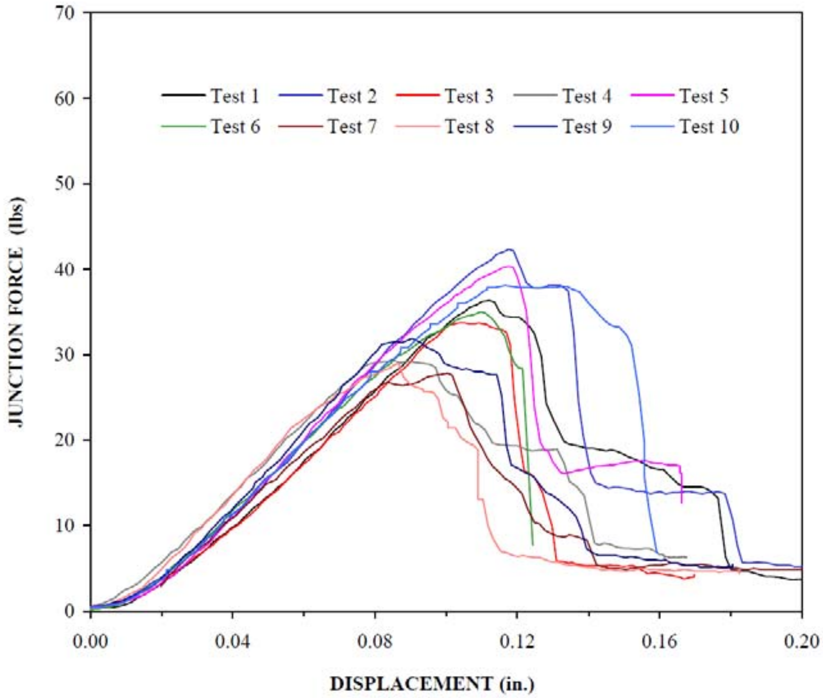

Figure D-5: Synteen SF 12.

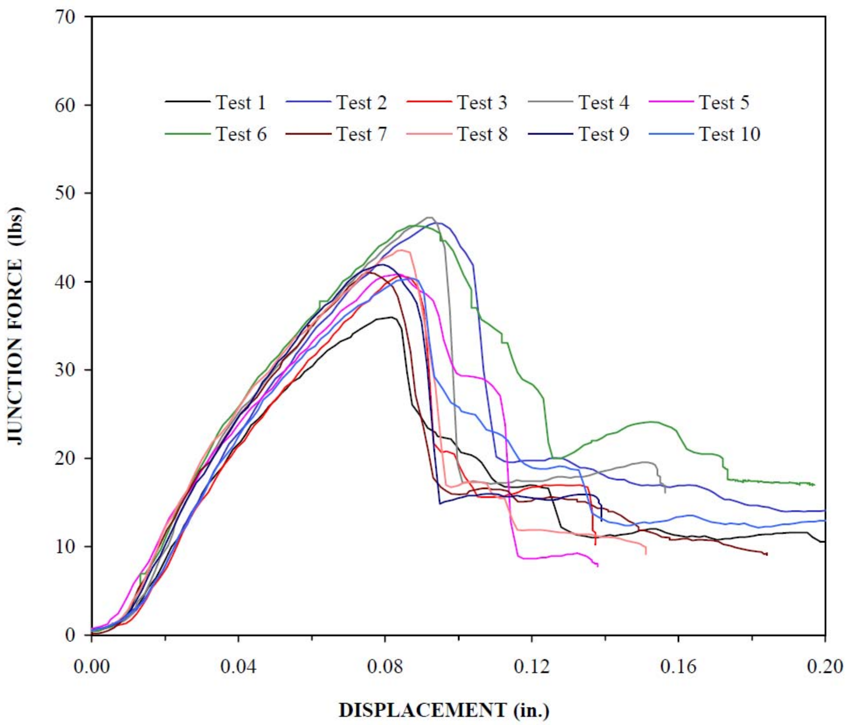

Figure D-6: TenCate Mirafi BXG 11.

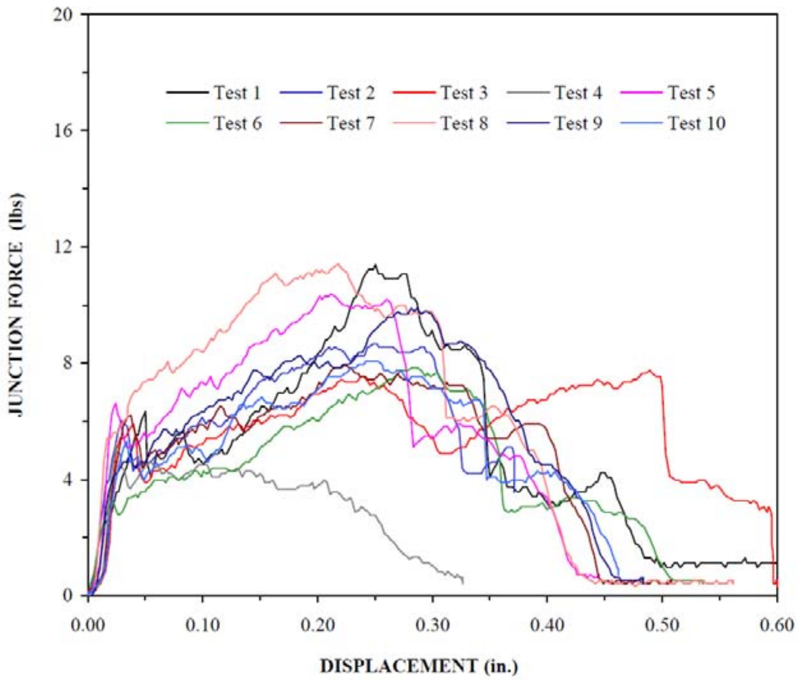

Figure D-7: Huesker Fornit 30.

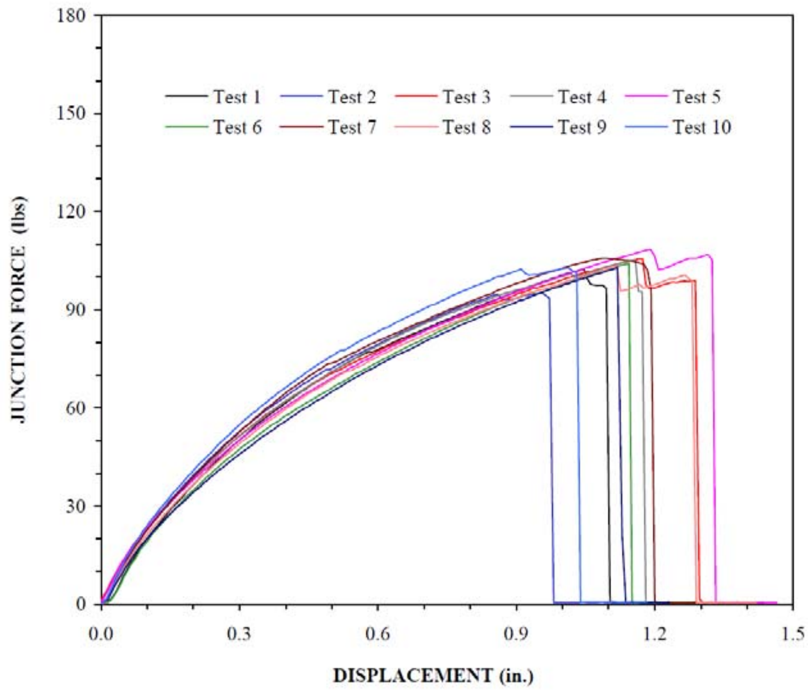

Figure D-8: SynTec Tenax MS330.

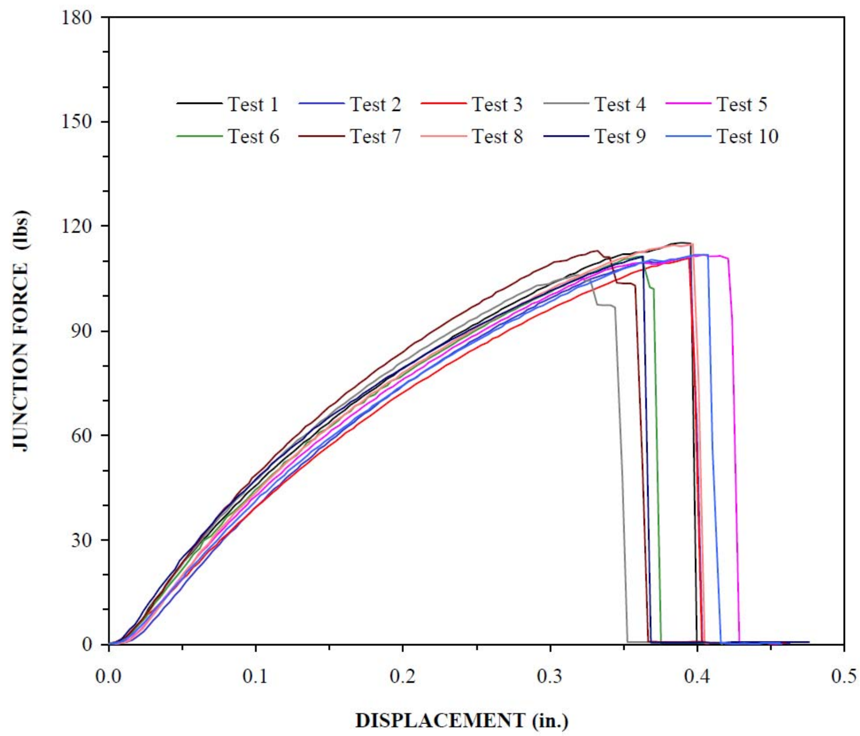

Figure D-9: Tensar TX 140.

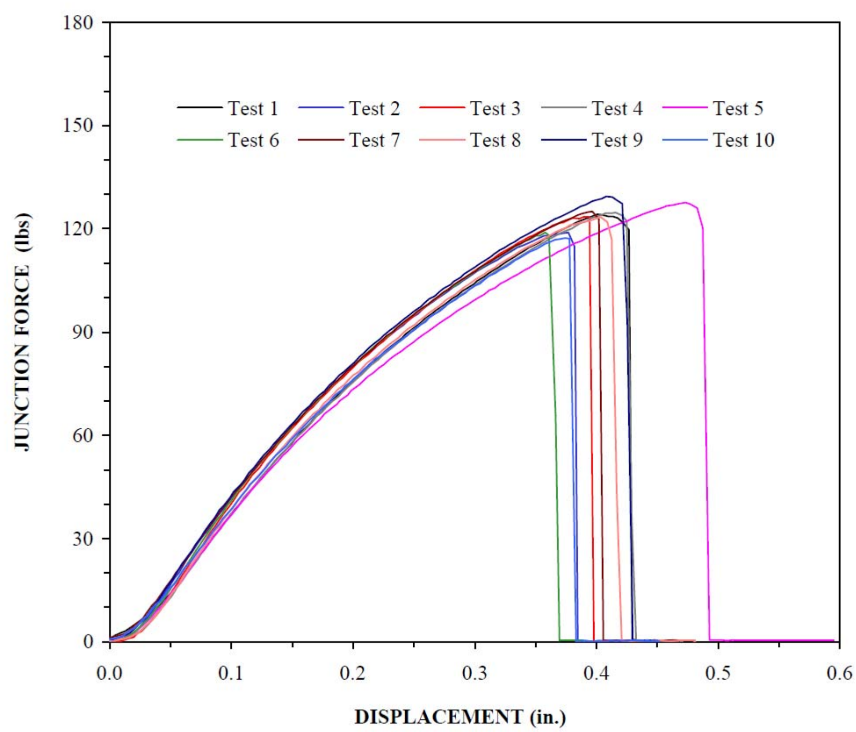

Figure D-10: Tensar TX 160.

Appendix E–Aperture Stability Modulus Plots

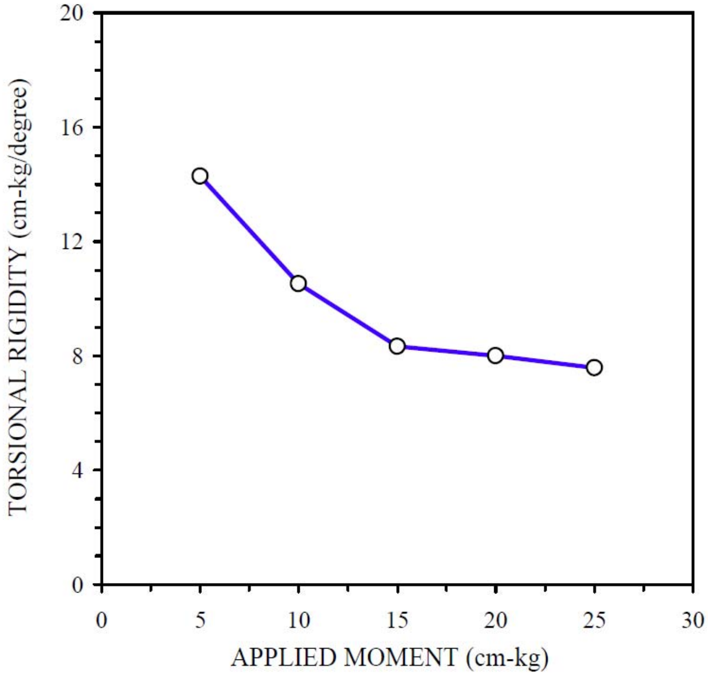

Figure E-1: Tensar BX Type 2.

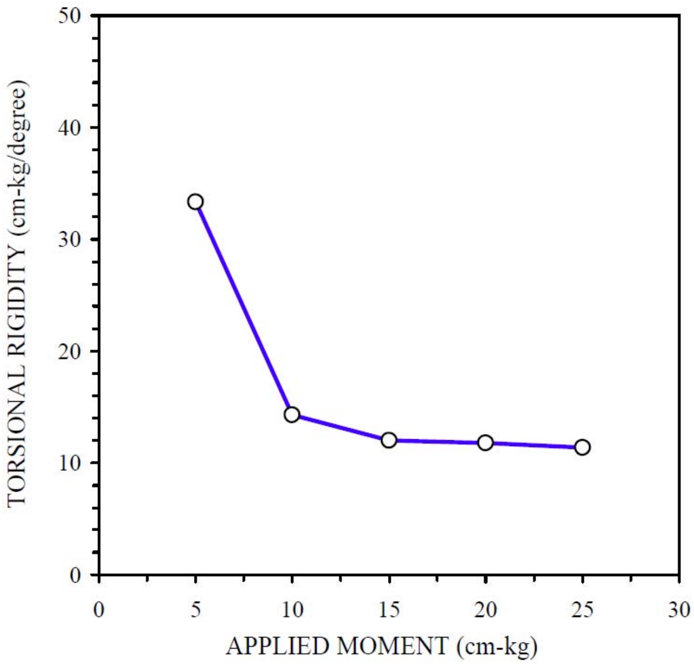

Figure E-2: NAUE Secugrid 30/30 Q1.

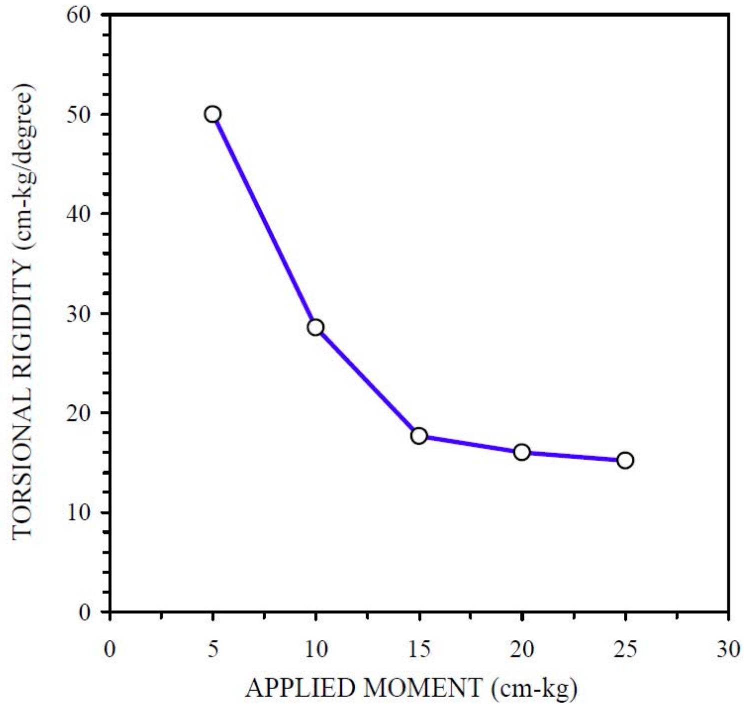

Figure E-3: Colbond Enkagrid Max 30.

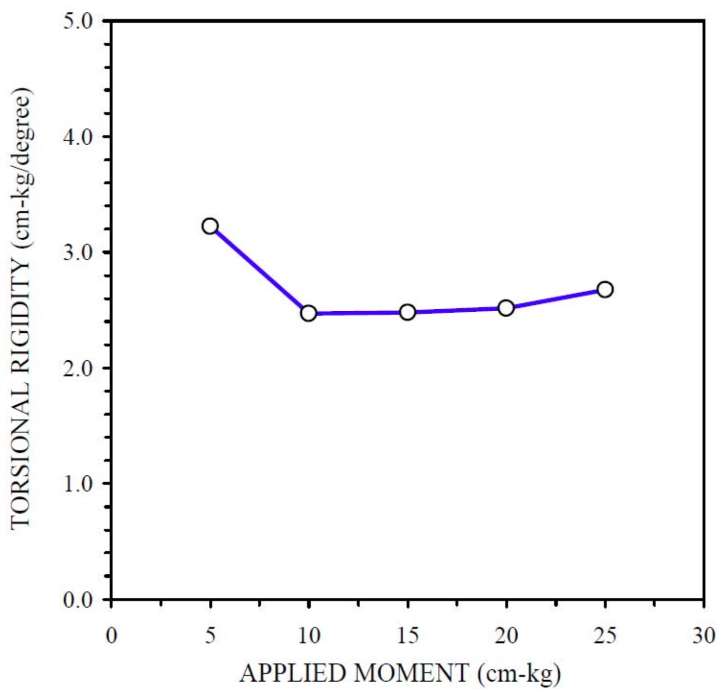

Figure E-4: Synteen SF 11.

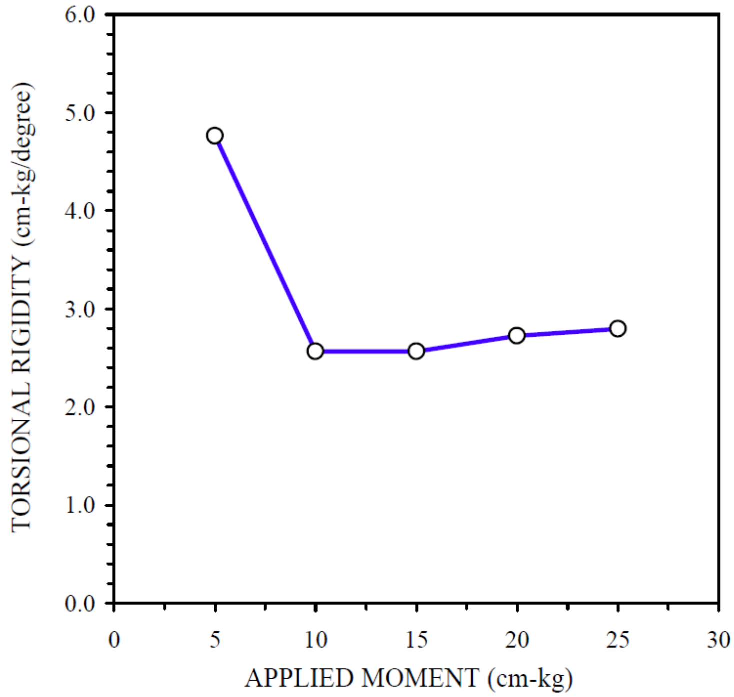

Figure E-5: Synteen SF 12.

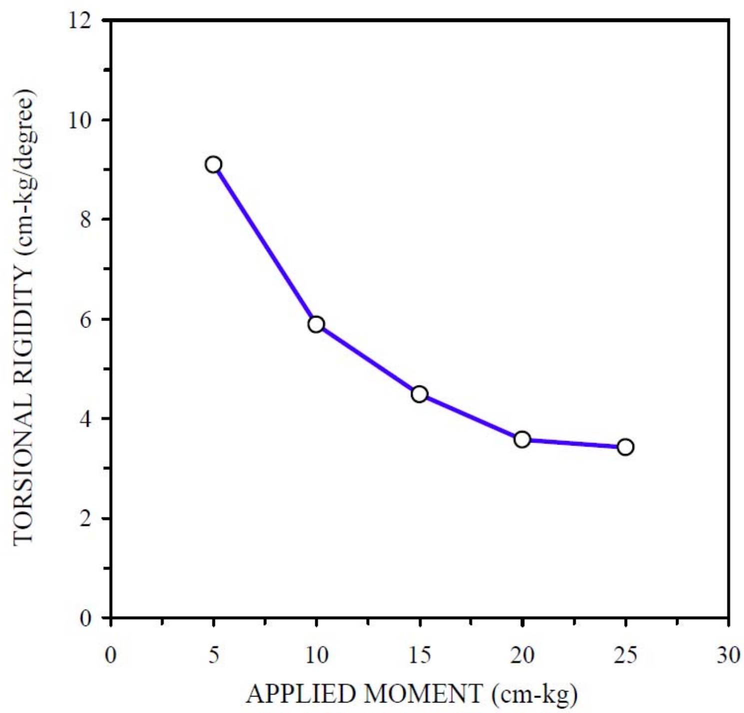

Figure E-6: TenCate Mirafi BXG 11.

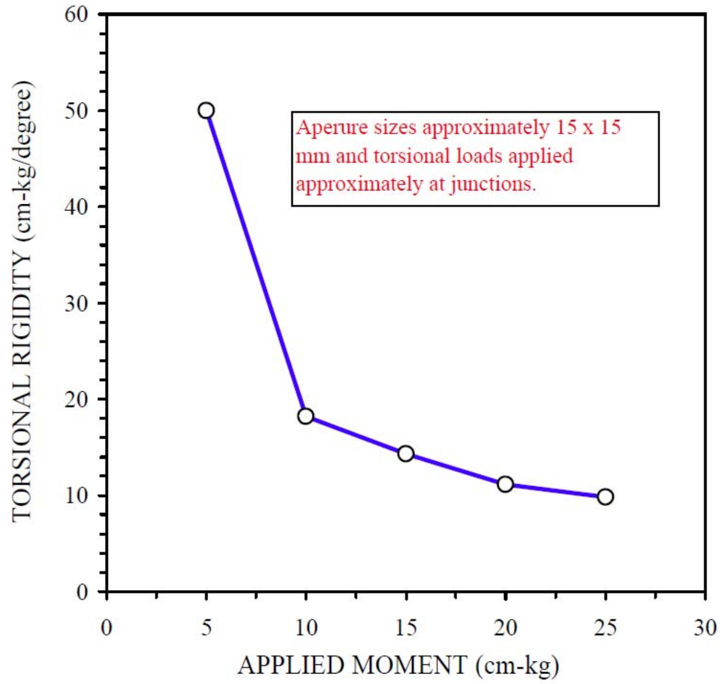

Figure E-7: Huesker Fornit 30.

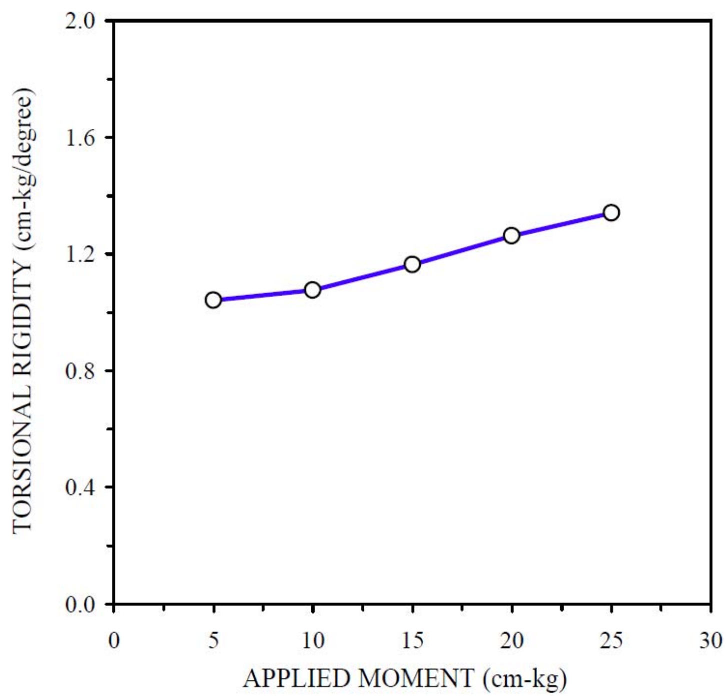

Figure E-8: SynTec Tenax MS330.

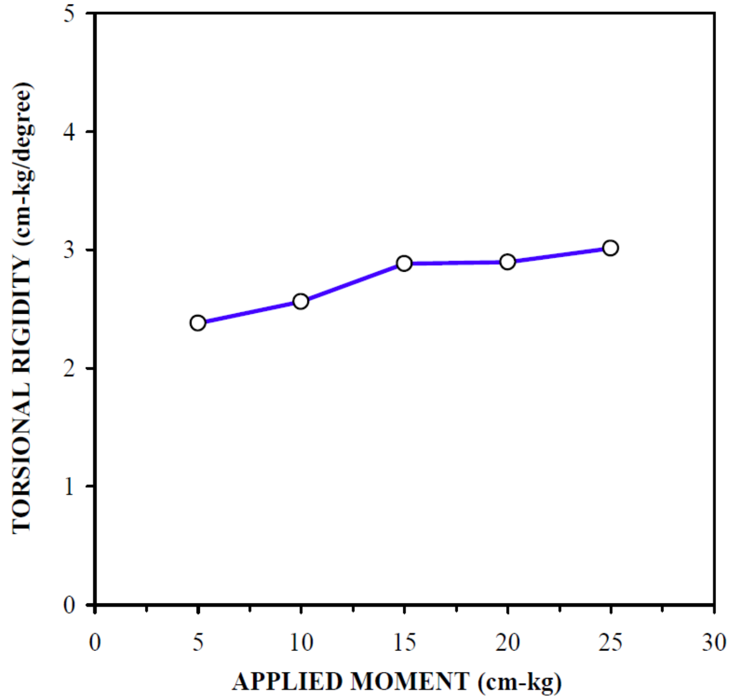

Figure E-9: Tensar TX 140.

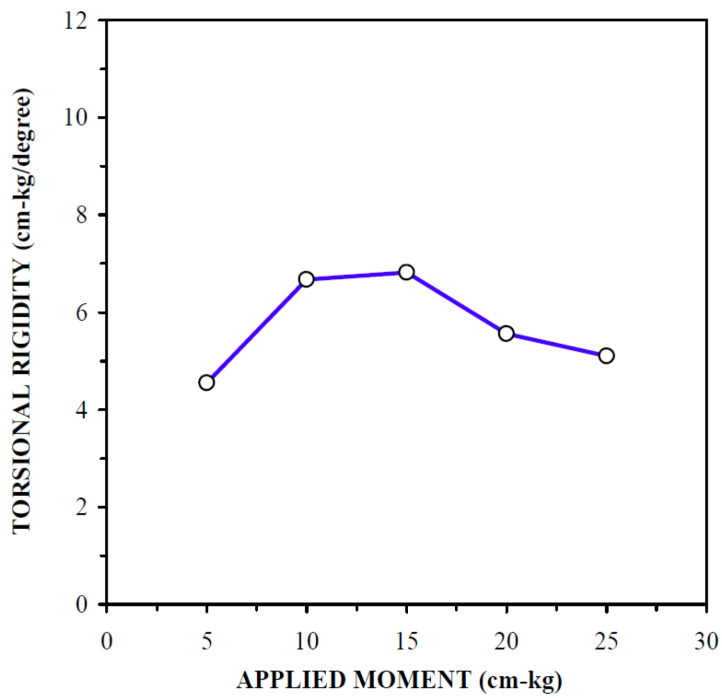

Figure E-10: Tensar TX 160.